

Generating Weighted MAX-2-SAT Instances of Tunable Difficulty with Frustrated Loops

Yan Ru Pei, Haik Manukian, and Massimiliano Di Ventra

Abstract—Many optimization problems can be cast into the maximum satisfiability (MAX-SAT) form, and many solvers have been developed for tackling such problems. To evaluate the performance of a MAX-SAT solver, it is convenient to generate difficult MAX-SAT instances with solutions known in advance. Here, we propose a method of generating weighted MAX-2-SAT instances inspired by the frustrated-loop algorithm used by the quantum annealing community to generate Ising spin-glass instances with nearest-neighbor coupling. Our algorithm is extended to instances whose underlying coupling graph is general, though we focus here on the case of bipartite coupling, with the associated energy being the restricted Boltzmann machine (RBM) energy. It is shown that any MAX-2-SAT problem can be reduced to the problem of minimizing an RBM energy over the nodal values. The algorithm is designed such that the difficulty of the generated instances can be tuned through a central parameter known as the frustration index. Two versions of the algorithm are presented: the random- and structured-loop algorithms. For the random-loop algorithm, we provide a thorough theoretical and empirical analysis on its mathematical properties from the perspective of frustration, and observe empirically, using simulated annealing, a double phase transition behavior in the difficulty scaling behavior driven by the frustration index. For the structured-loop algorithm, we show that it offers an improvement in difficulty of the generated instances over the random-loop algorithm, with the improvement factor scaling super-exponentially with respect to the frustration index for instances at high loop density. At the end of the paper, we provide a brief discussion of the relevance of this work to the pre-training of RBMs.

I. INTRODUCTION

A maximum-satisfiability (MAX-SAT) problem is an optimization problem where the objective is to find the truth values of literals (boolean variables or their negation) in a boolean formula in conjunctive normal form (CNF) such that the number of satisfied clauses is maximized [1]. A Max-2-SAT problem is a Max-SAT problem with at most 2 literals (i.e., variables or their negation) per clause [2]. Many optimization problems can be reduced to this particular problem [3]–[5], making it a valuable testing ground for various algorithms/solvers. In this paper, we focus on the weighted MAX-2-SAT problem, which is a more general version of the MAX-2-SAT problem where each clause is assigned with some non-negative weight [1], and the objective is to find the truth assignments of the literals that maximizes the combined weight of the satisfied clauses.

The optimization version of the (weighted) MAX-2-SAT problem is known to be NP-hard [6], and it is difficult to

check whether a solver has found the optimal solution for a given instance. This makes the evaluation of the performance of a MAX-SAT solver rather impractical. An algorithm that generates Max-2-SAT instances of tunable difficulty such that the solution is known in advance (planted solution) would therefore be very beneficial. Such algorithms exist, but they generally suffer from one or more of the following drawbacks: they are unable to generate sufficiently hard instances [7], the planted solution is not necessarily the optimal solution [8], they are limited in the structures of the instances that they can generate [9], or they require a considerable amount of computational time to generate the instances [10].

In this paper, we introduce an algorithm that is capable of generating weighted Max-2-SAT instances of tunable difficulty in both the low and high clause density regimes and does not suffer from the above limitations. For ease of theoretical analysis and empirical studies, we can reduce a given weighted MAX-2-SAT problem into the following problem (see Section II)

$$\begin{aligned} &\text{Find a configuration of } \mathbf{v} \in \{0, 1\}^n \text{ and } \mathbf{h} \in \{0, 1\}^m \\ &\text{such that the following energy function is minimized:} \quad (1) \\ &E(\mathbf{v}, \mathbf{h}) = -\left(\sum_{ij} W_{ij} v_i h_j + \sum_i a_i v_i + \sum_j b_j h_j\right). \end{aligned}$$

where $\mathbf{a} \in \mathbb{R}^n$, $\mathbf{b} \in \mathbb{R}^m$, and $\mathbf{W} \in \mathbb{R}^{n \times m}$ are real numbers. This is essentially an optimization problem over some binary variables partitioned into two disjoint sets, so the underlying graph of the problem is bipartite. A boolean optimization problem of this type can always be reduced to a bipartite form [11] (see Section II-B), so it is sufficient for us to focus on instances with a bipartite structure. However, this reduction involves doubling the number of boolean variables and introducing clauses of large weights, thus introducing unnecessary computational and memory burden in a practical implementation of the algorithm. Therefore, it will still be useful to have an algorithm that is able to directly generate instances of any structure. Even though in this paper we only focus on generating bipartite instances, our algorithm can be easily extended to instances of any structure (see Section IV-H).

The quantity $E(\mathbf{v}, \mathbf{h})$ is also called the *RBM energy* in the field of machine learning, because it is the energy function for a restricted Boltzmann machine (RBM) [12]. For this reason, we can also call a weighted Max-2-SAT problem an *RBM instance*. Finding the minimum RBM energy (or *RBM ground state*) is an important problem, because the ground state configuration corresponds to the mode of the RBM joint probability distribution [12, 13]. Finding the mode of this

YRP, HM, and MD are with the Department of Physics, University of California-San Diego, 9500 Gilman Drive, La Jolla, California 92093-0319, USA, (e-mail: yrpei@ucsd.edu, hmanukia@ucsd.edu, diventra@physics.ucsd.edu).

distribution allows for a much more efficient sampling of the RBM model distribution [14]–[16], which helps improve the RBM pre-training in both decreasing the number of iterations to convergence [17, 18] and minimizing the KL-divergence [19]. A brief extension of this discussion will be presented in Section VII, and a more thorough treatment of this topic will be given in another work [20].

To generate RBM instances with a known global optimum and tunable difficulty, we take inspiration from the *frustrated-loop algorithm* used by the quantum annealing community to benchmark the performance of their quantum annealers [9]. However, due to the high connectivity and non-local coupling nature of the RBM instance, the frustrated-loop algorithm in its original form is unable to provide sufficient difficulty for large instances. Instead, by enforcing certain *structures* on the loops (see Section V) we can retain the hardness as we increase the connectivity of the system.

The paper is organized as follows. In Section II, we show the reduction of a general weighted MAX-2-SAT problem into an Ising spin-glass problem [21] of bipartite form. In Section III, we introduce the *frustration index* [22] in the context of a *gauged RBM*, and discuss its connection to the population of local minima. In Section IV, we introduce the *random frustrated loop algorithm* and propose a general method for direct control of the frustration index. We also investigate some of its interesting mathematical properties, and discuss the limitations of the algorithm in its original form. In Section V, we make improvements on the algorithm by giving the loops certain geometrical structures, and we name the new algorithm *structured loop algorithm*. We show analytically that the new algorithm has the ability to generate difficult instances at high loop density. In Section VI, we study empirically how the difficulties of the generated instances scale with RBM size, frustration index, and loop density. We observe the *hardness peaks* [23] with respect to the loop density for systems of different sizes, and discover a double phase transition behavior [24] in the difficulty scaling behavior driven by the frustration index. Furthermore, as the frustration index is tuned, we observe a doubly exponential scaling behavior in the difficulty improvement from the random to structured loop algorithms. In Section VII, we offer a brief discussion on the practical and heuristic connections of this work to the task of pre-training an RBM.

The scripts for generating the instances using the random and structured loop algorithms and solving the instances using simulated annealing (SA) are written in MATLAB, and they are accessible through GitHub (<https://github.com/PeaBrane/Loop-Algorithm.git>) [25].

II. FROM WEIGHTED MAX-2-SAT TO BIPARTITE SPIN GLASS

The goal of this Section is to show that any given weighted MAX-2-SAT instance can be reduced to an energy minimization problem over a bipartite spin glass with spin values $\{-1, 1\}$, that can be generated by using the frustrated-loop algorithm. Note that this reduction implies that the bipartite spin-glass energy minimization problem is at least as hard as

the weighted MAX-2-SAT problem [26], so one can effectively test the performance of a weighted MAX-2-SAT solver on the corresponding bipartite spin-glass problem.

The reduction is done in three stages. First, we reduce a general weighted MAX-2-SAT instance into a quadratic binary optimization (QUBO) problem [27]. Then, we reduce the QUBO problem into a larger QUBO problem of the bipartite form. Finally, we convert the binary node values of $\{0, 1\}$ into $\{-1, 1\}$, and introduce two extra spins to represent the biases.

A. From Weighted MAX-2-SAT to QUBO

QUBO is the problem of maximizing the following quadratic polynomial

$$\sum_{i=1}^n B_i x_i + \sum_{i=1}^n \sum_{j>i}^n Q_{ij} x_i x_j, \quad (2)$$

over the binary variables $\mathbf{x} \in \{0, 1\}^n$, with the coefficients B_i and Q_{ij} being real numbers.

The reduction from a weighted MAX-2-SAT problem to a QUBO problem is rather straightforward, and it simply involves converting each clause into the equivalent QUBO form

$$\begin{aligned} (x_i \vee x_j) &\rightarrow x_i + x_j - x_i x_j, \\ (\neg x_i \vee x_j) &\rightarrow 1 - x_i + x_i x_j, \\ (x_i \vee \neg x_j) &\rightarrow 1 - x_j + x_i x_j, \\ (\neg x_i \vee \neg x_j) &\rightarrow 1 - x_i x_j. \end{aligned}$$

Note that a negation of x_i is expressed as $1 - x_i$. Then we simply sum all the terms corresponding to all the clauses with their respective weights, and the resulting expression is in the QUBO form after ignoring the constant offset. It is not hard to see that maximizing the summed weights of the satisfied clauses is equivalent to maximizing the quadratic polynomial in Eq. (2).

B. Bipartite Conversion

A general QUBO problem of the bipartite form involves partitioning the binary variables into two disjoint sets \mathbf{v} and \mathbf{h} , with every quadratic term in the polynomial only containing variables from the two different sets

$$\sum_{i=1}^n a_i v_i + \sum_{j=1}^m b_j h_j + \sum_{i=1}^n \sum_{j=1}^m W_{ij} v_i h_j, \quad (3)$$

where $\mathbf{v} \in \{0, 1\}^n$ and $\mathbf{h} \in \{0, 1\}^m$. Note that the underlying bipartite graph is $K_{n,m}$ [11] for this general bipartite QUBO problem.

For a given QUBO problem of the general form (Eq. (2)), we can take its underlying bipartite graph to be $K_{n,n}$, and the goal is to find the bipartite polynomial such that the truth assignment of \mathbf{v} that maximizes it corresponds exactly to the truth assignment of \mathbf{x} that maximizes the original polynomial. A possible bipartite polynomial that accomplishes this is

$$\sum_{i=1}^n B_i v_i + \sum_{i=1}^n \sum_{j>i}^n Q_{ij} v_i h_j + C(\mathbf{v}, \mathbf{h}), \quad (4)$$

with $C(\mathbf{v}, \mathbf{h})$ some function of the variables. Note that the first two terms in Eq. (4) constitute a less general bipartite polynomial than Eq. (3) because all the linear coefficients of \mathbf{h} are set to zero, and all the quadratic coefficients with $i \geq j$ are set to zero. If we were to enforce the constraint that $\mathbf{v} = \mathbf{h}$ at the maximum of the polynomial, then it is not hard to see that maximizing this polynomial and maximizing the polynomial in Eq. (2) are equivalent problems under this constraint. This constraint is in fact enforced by the third term $C(\mathbf{v}, \mathbf{h})$.

The purpose of the constraint term is to introduce a large penalty whenever $\mathbf{v} \neq \mathbf{h}$, so that we are guaranteed that $\mathbf{v} = \mathbf{h}$ at the maximum of the polynomial. A possible choice of $C(\mathbf{v}, \mathbf{h})$ is the following

$$C(\mathbf{v}, \mathbf{h}) = 2 \left(\sum_{i=1}^n |B_i| + \sum_{i=1}^n \sum_{j>i}^n |Q_{ij}| \right) \sum_{i=1}^n (1 + 2v_i h_i - v_i - h_i),$$

where $1 + 2v_i h_i - v_i - h_i$ is equivalent to an XNOR operation [28] between v_i and h_i that returns a 1 if v_i and h_i are the same and a 0 if v_i and h_i are different. The coefficient is the sum of the absolute values of all the weights in the original QUBO problem. This constraint function guarantees that $\mathbf{v} = \mathbf{h}$ at the maximum of the polynomial in Eq. (4), which is also the assignment of \mathbf{x} that maximizes the polynomial in Eq. (2) (see Appendix A for a formal proof of these two statements), which shows the equivalence of the two QUBO problems.

It should be noted that the bipartite QUBO polynomial (Eq. (3)) is simply the RBM energy (Eq. (1)) with a difference of a minus sign, so the problem of maximizing the bipartite QUBO polynomial is the same as minimizing the RBM energy.

C. Conversion to $\{-1, 1\}$ Binary Values

In the original formulation of the RBM energy (Eq. (1)), the binary values of the variables are set to $\{0, 1\}$ for a direct correspondence with the boolean values. However, this restriction is unnecessary, and we can choose the binary values to be any two distinct numbers. For the sake of this paper, we map the binary values $\{\mathbf{v}, \mathbf{h}\} \in \{0, 1\}^{n+m}$ into the binary values $\{\mathbf{v}', \mathbf{h}'\} \in \{-1, 1\}^{n+m}$ so that the quadratic terms in the RBM energy can be interpreted as Ising spin couplings. The conversion to the $\{-1, 1\}$ values can be simply performed as follows

$$\mathbf{v}' = -1 + 2\mathbf{v}, \quad \mathbf{h}' = -1 + 2\mathbf{h}.$$

With this conversion, the RBM energy can be written in terms of the new binary values as

$$\begin{aligned} E(\mathbf{v}', \mathbf{h}') &= - \left(\sum_{i=1}^n a_i \frac{v'_i + 1}{2} + \sum_{j=1}^m b_j \frac{h'_j + 1}{2} \right. \\ &\quad \left. + \sum_{i=1}^n \sum_{j=1}^m W_{ij} \frac{v'_i + 1}{2} \frac{h'_j + 1}{2} \right) \\ &= - \sum_{i=1}^n \frac{1}{2} (a_i + \sum_{j=1}^m W_{ij}) v'_i \\ &\quad - \sum_{j=1}^m \frac{1}{2} (b_j + \sum_{i=1}^n W_{ij}) h'_j - \sum_{i=1}^n \sum_{j=1}^m \frac{W_{ij}}{4} v'_i h'_j \\ &\quad - \left(\sum_{i=1}^n \frac{a_i}{2} + \sum_{j=1}^m \frac{b_j}{2} + \sum_{i=1}^n \sum_{j=1}^m \frac{W_{ij}}{4} \right). \end{aligned}$$

We can define the new linear and quadratic coefficients to be $a'_i = \frac{1}{2}(a_i + \sum_j W_{ij})$, $b'_j = \frac{1}{2}(b_j + \sum_i W_{ij})$, and $W'_{ij} = \frac{W_{ij}}{4}$, respectively. Furthermore, we can choose to ignore the last bracketed term since it is just a constant offset independent of the $\{\mathbf{v}', \mathbf{h}'\}$. The RBM energy can then be rewritten as

$$E'(\mathbf{v}', \mathbf{h}') = - \left(\sum_{i=1}^n a'_i v'_i + \sum_{j=1}^m b'_j h'_j + \sum_{i=1}^n \sum_{j=1}^m W'_{ij} v'_i h'_j \right).$$

We thus see that the form of the RBM energy is invariant under the conversion of binary values. For the rest of the paper, we will always assume we are using the $\{-1, 1\}$ node values, so we can drop the prime symbols for clarity, and simply denote \mathbf{v} as the *visible spins* and \mathbf{h} as the *hidden spins* in accordance with the RBM terminology [12].

D. Biases as Ghost Spins

The linear coefficients in the RBM energy are usually called *biases*. The bias terms can be interpreted as spins interacting with some external field [21]. In some cases, it is convenient to express this interaction as a two-body interaction between a spin and some imaginary fixed spin, or *ghost spins* [29] with a coupling strength proportional to the external field.

To be more precise, we can define additional weight elements $W_{i,m+1} = a_i$ and $W_{n+1,j} = b_j$. Furthermore, we set $v_{n+1} = 1$ and $h_{n+1} = 1$. Then the RBM energy can be written compactly as

$$E(\mathbf{v}, \mathbf{h}) = - \sum_{i=1}^{n+1} \sum_{j=1}^{m+1} W_{ij} v_i h_j.$$

In this form, the linear terms are completely absorbed as quadratic terms, and the expression is fully quadratic.

III. FRUSTRATION OF RBMS

In this Section we formulate an RBM instance entirely in terms of its corresponding *weight matrix*, and express the actions of spin flips as *vertex switching* [30], which corresponds to negating the signs of a certain subset of weight elements. We then introduce a difficulty measure known as the *frustration index* [21, 22] and discuss its relationship to the population of

local minima of the RBM instance. For simplicity, we assume for the rest of the paper that the RBM model is *unbiased* [12] (unless specifically mentioned). In other words, we set $\mathbf{a} = 0$ and $\mathbf{b} = 0$. Note that most of the arguments can be easily generalized to a *biased* RBM.

A. Vertex Switching

Given any spin configuration $\mathbf{s} = \{\mathbf{v}, \mathbf{h}\}$ of the RBM, we can negate the signs of (or flip) some subset of spins and arrive at some new configuration $\mathbf{s}' = \{\mathbf{v}', \mathbf{h}'\}$. Similarly, we can also start from some RBM weight matrix \mathbf{W} , and negate some subset of weight elements and arrive at some new weight matrix \mathbf{W}' . For every subset of negated spins, there is a corresponding subset of weights that we can negate such that the RBM energy remains invariant for every configuration \mathbf{s} . This transformation is called *vertex switching* in the language of graph theory [30].

Given any pair of configurations $\mathbf{s} = \{\mathbf{v}, \mathbf{h}\}$ and $\mathbf{s}' = \{\mathbf{v}', \mathbf{h}'\}$, we can then define $I(v, v') = \{i | v_i \neq v'_i\}$, or the set of different visible spins between the two configurations. Similarly, we define $J(h, h') = \{j | h_j \neq h'_j\}$, the set of different hidden spins. Furthermore, we define the complement of $I(v, v')$ as $I(v, v')^c = [n]/I(v, v') = \{i | v_i = v'_i\}$, and $J(h, h')^c = [m]/J(h, h') = \{j | h_j = h'_j\}$. Note that $[n]$ denotes all integers from 1 to n , or all the visible spin indexes. Then we see that the energy of the spin state \mathbf{s}' can be expressed as follows

$$\begin{aligned} E(\mathbf{s}') &= - \sum_{ij} W_{ij} v'_i h'_j \\ &= - \sum_{I, J} W_{ij} (-v_i) (-h_j) - \sum_{I, J^c} W_{ij} v_i (-h_j) \\ &\quad - \sum_{I^c, J} W_{ij} (-v_i) h_j - \sum_{I^c, J^c} W_{ij} v_i h_j \\ &= - \left(\sum_{I, J} W_{ij} v_i h_j + \sum_{I^c, J^c} W_{ij} v_i h_j \right) \\ &\quad + \left(\sum_{I, J^c} W_{ij} v_i h_j + \sum_{I^c, J} W_{ij} v_i h_j \right). \end{aligned}$$

For convenience, we define the corresponding *switching subset* of the index pairs to be $F = \{\{i, j\} | (i \in I \wedge j \in J) \vee (i \in I^c \wedge j \in J)\}$, and we let its complement be $F^c = \{\{i, j\} | (i \in I \wedge j \in J) \vee (i \in I^c \wedge j \in J^c)\}$ (see Figure 1 for a visual representation of this set). Therefore, if we were to simultaneously negate the weight elements with indexes in this set F , then the new energy would be

$$\begin{aligned} E'(\mathbf{s}') &= - \sum_{F^c} W_{ij} v_i h_j + \sum_F (-W_{ij}) v_i h_j \\ &= - \sum_{ij} W_{ij} v_i h_j = E(\mathbf{s}), \end{aligned}$$

which implies the invariance of the RBM energy under the simultaneous spin flips and corresponding weight flips.

Note that we can construct F from any pair of I and J . However, the reverse is not true. If we negate any arbitrary subset of weight elements, it may be not possible to find the subset of spins in I, J such that the RBM energy remains

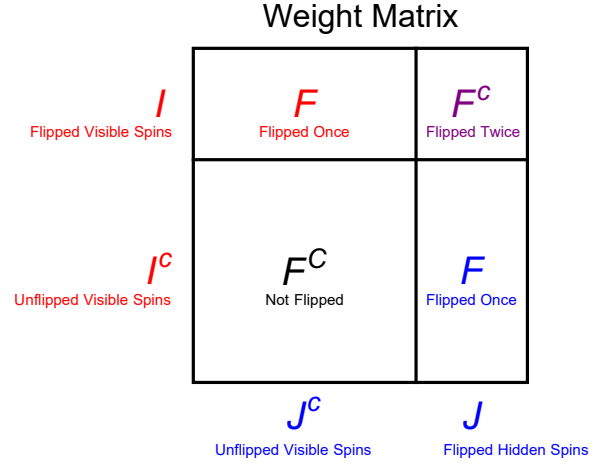


Fig. 1: Vertex switching illustrated in terms of the weight matrix. The elements in the lower-left block are not flipped. The elements in the upper-left and lower-right blocks are flipped once. The elements in the upper-right block are flipped twice, hence remain the same.

invariant. If the weight matrices of two RBMs are related by F corresponding to some I and J , then we say that the two RBMs are *vertex-switching equivalent* [30]. We can think of F as the set of weight edges with one end in I and the other end in J^c , or one end in J and the other end in I^c . This makes sense because switching a vertex necessarily implies the negation of the signs of all the weights connected to it, so if an edge is connected to only one switched vertex, its sign will be negated; however, if the edge is connected to two switched vertices, then its sign will be negated twice, or simply remain the same.

Given any transformation from state \mathbf{s} to \mathbf{s}' , we have a unique corresponding pair of I and J , so we can construct $F(I, J)$ solely in terms of \mathbf{s} and \mathbf{s}' . It is easy to see that the inverse transformation from \mathbf{s}' to \mathbf{s} corresponds to the same pair of I and J as the forward transformation, hence the associated switching subset $F(\mathbf{s}', \mathbf{s})$ is also the same. Simply put, $F(\mathbf{s}, \mathbf{s}') = F(\mathbf{s}', \mathbf{s})$, and the forward and inverse transformations have the same corresponding switching subset F .

It is easy to see that negating the spins in I, J (while keeping the weight matrix the same) is equivalent to negating the weight elements in F (while keeping the spins the same). So if we know the energy of some spin state \mathbf{s} and wish to find the energy of another spins state \mathbf{s}' , we can keep the spin state fixed at \mathbf{s} and negate the corresponding switching subset $F(\mathbf{s}, \mathbf{s}')$ of weight elements

$$\begin{aligned} E(\mathbf{s}') &= - \sum_{F^c} W_{ij} v_i h_j - \sum_F (-W_{ij}) v_i h_j \\ &= - \sum_{F^c \cup F} W_{ij} v_i h_j + 2 \sum_F W_{ij} v_i h_j \\ &= E(\mathbf{s}) + 2 \sum_F W_{ij} v_i h_j. \end{aligned} \tag{5}$$

B. Metric

It is useful to define some form of distance/metric [31] between two states on an RBM, so we have some sense of how “different” or “far apart” the two states are. A naïve choice would be to count the number of spins that are different between the two states, or the so-called “Manhattan distance” [32]. But this measure is not particularly insightful, because given some state, we can flip all the spins and arrive at a different state that is seemingly “far” from the original state. However, the action of flipping all the spins is equivalent to flipping the signs of the biases, which has a small contribution to the structure of the RBM (or no contribution at all in the case of an unbiased RBM). Therefore, a possible solution is to use the cardinality [33] of the vertex-switching subset $|F|$ as a measure of distance.

If we assume all the weight elements \mathbf{W} and spins \mathbf{s} are independent random variables, where \mathbf{W} consists of identical, independent random variables [13] with mean μ and standard deviation σ , then v_i or h_j have equal probabilities to be in the $+1$ and -1 states. Then it is easy to show the following (see Appendix B)

$$\text{var}(E(\mathbf{s}') - E(\mathbf{s})) = 4|F(\mathbf{s}, \mathbf{s}')|(\mu^2 + \sigma^2),$$

where $|F(\mathbf{s}, \mathbf{s}')|$ is the cardinality of the flipped subset. We see that the variance of the energy difference between the \mathbf{s} and \mathbf{s}' states scales linearly with $|F(\mathbf{s}, \mathbf{s}')|$, so it is natural for us to define the metric between two states as follows

$$d(\mathbf{s}, \mathbf{s}') = \frac{|F(\mathbf{s}, \mathbf{s}')|}{nm},$$

where $|F(\mathbf{s}, \mathbf{s}')|$ can be expressed as

$$|F(\mathbf{s}, \mathbf{s}')| = n_v m + n m_h - 2n_v m_h,$$

and n_v is the number of visible spins flipped, while m_h is the number of hidden spins flipped. The denominator serves just to normalize the distance such that $d \leq 1$. This distance gives us a sense of how “different” the two states are, since the greater the distance, the more uncertainty in the energy difference. From here, it can be easily shown that $d(\mathbf{s}, \mathbf{s}')$ is in fact a true metric for the case of a biased RBM (see Appendix C). For an unbiased RBM, if we assume that any two states related by a global spin flip are the same state (Z_2 symmetry [34]), then d is also a true metric.

C. Gauged RBM

Consider now an RBM with some ground state configuration \mathbf{s}_0 . We can always flip a particular subset of spins such that the \mathbf{s}_0 state becomes the $+1$ state (the spin state with all spins being $+1$). Therefore, we can flip the corresponding vertex-switching subset of weight elements such that the new RBM is vertex-switching equivalent to the original RBM. The new weight matrix describes an RBM with the ground state being the $+1$ state, and we call this RBM a “gauged RBM”. This name is inspired by the similar technique of gauge transforming a spin-glass model such that the ground state is the $+1$ state [35].

Note that we can generate the set of all RBM configurations with the set of all gauged RBM through the switching

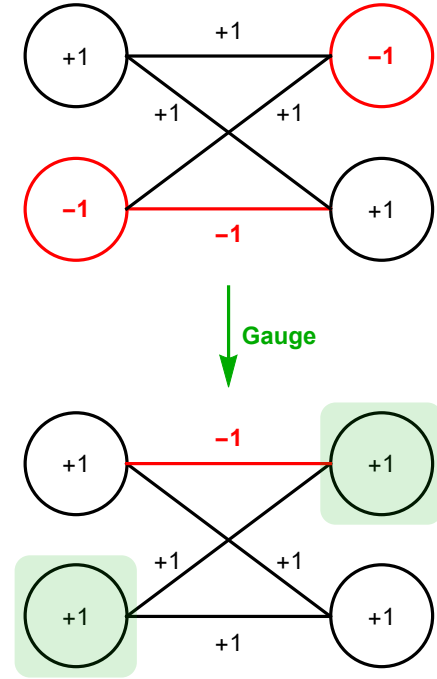


Fig. 2: Transforming a 2×2 RBM with into a gauged RBM through vertex-switching. Note that the new ground is the $+1$ state, and edges with only one end connected to the switched vertices are flipped.

operation. This is because the switching operation is invertible and any RBM can be transformed into a gauged RBM through switching the ground state to the $+1$ state through the switching subset $F(\mathbf{s}_0, +1)$, then the same switching subset can be used to perform the inverse gauge transformation to recover the original RBM weight matrix (see Section III-A).

Consider a gauged RBM with weights \mathbf{W} , then the ground state energy is simply the sum of all the weight elements

$$E(+1) = - \sum_{i,j} W_{ij} v_i h_j = - \sum_{i,j} W_{ij} (+1)(+1) = - \sum_{i,j} W_{ij}.$$

From Eq. (5) we see that any other state \mathbf{s} can be simply expressed as

$$E(\mathbf{s}) = E(+1) + 2 \sum_F W_{ij}.$$

From this expression, we see that the energy gap between an arbitrary state and the ground state is proportional to the sum of the weight elements in the corresponding switching subset. Note that for a gauged RBM, the sum of the weight elements of the switching subset must be positive, otherwise we would be able to obtain a configuration with a lower energy than the ground state configuration. We call this the *positive-sum condition*, and it can be used to check whether an RBM is gauged or not. Recall that not every subset of the weight elements can be realized as a switching subset, so it is not necessarily true that the sum of any subset of weight elements must be positive.

In practice, it is convenient to first generate the gauged RBM weight matrix by ensuring that the ground state is kept at $+1$

(see Section IV-B), and then the weight matrix can be later processed to have any given spin configuration \mathbf{s}_0 as the ground state by simply taking the inverse gauge transformation. The MATLAB implementation of this inverse gauge transformation is available as the script `gauge_inverse.m` in the GitHub repository [25].

D. Frustration

In the language of graph theory, the frustration index of a weighted graph is usually defined as the ratio between the sum of the magnitudes of the unsatisfied bonds at the ground state and the sum of the magnitudes of all the bonds [22]. In the case of a gauged RBM, it is easy to see that a positive weight element denotes a satisfied bond and a negative weight element denotes an unsatisfied bond, so we can define the frustration index of an RBM to be simply the sum of the absolute values of all the negative weight elements and the sum of the absolute values of all weight elements

$$f = \frac{-\sum_{W_{ij} < 0} W_{ij}}{\sum |W_{ij}|} = \frac{1}{2} \frac{\sum |W_{ij}| - \sum W_{ij}}{\sum |W_{ij}|} \quad (6)$$

Note that for the special case where $f = 0$, all the weight elements are positive. In this case, the corresponding switching subset of the next lowest state is usually just a single row or a single column, corresponding to a small $|F|$ and a small sum of the weight elements $\sum_F W_{ij}$. Even though we are only flipping a single row/column, the energy gap can be relatively large because all the weight elements are positive.

Contrast the previous case with a case where f is large, or a gauged RBM with many negative weight elements. In this case, the switching subset F of the next lowest energy state, the first *excited state*, does not necessarily have to have a small cardinality because it is possible for the sum of the negative weight elements to almost cancel out the sum of the positive weight elements, resulting in a relatively small total sum (thus energy gap) even when the cardinality of the switching subset is large. In other words, for a highly frustrated system, the transition between the ground state and the excited states usually require small energy inputs but may require a large number of spin flips (corresponding to a large cardinality of the switching subset) [21].

E. Maximum Frustration

One interesting question is what maximum frustration can an RBM achieve. This question is not only of mathematical interest, but also of practical importance, since knowing the maximum frustration provides a baseline for evaluating the difficulty of the generated instances.

If we take an RBM instance to be the underlying bipartite graph of a quasirandom graph [36] such as a large Paley graph [37], then it can be shown that there is no constant upper bound to the frustration index except for the trivial 0.5. This can be shown as a corollary of the fourth theorem of a quasi-random graph stated and proved of Chung's paper [36].

However, the argument does not impose any restriction on the system size, and in practice, the system may have to be unrealistically large in order for the frustration index to be

near 0.5. A more practically useful question is then what the maximum frustration of an RBM of a given size is. In Appendix E, we provide a short proof that the maximum frustration is 0.25 for the special case of a $2 \times m$ RBM, which is exactly the maximum frustration that the loop algorithm is able to achieve (see Section IV-C).

F. Local Minima

The frustration index is closely related to the abundance of local minima [38]. This makes sense because in a highly frustrated system, there are usually many closely spaced high energy states related by large numbers of spin flips. So if the system ends up in one of these states, we cannot access a lower energy state by simply performing single-spin flips. This is usually referred to as being “stuck” in a local minima.

However, not all local minima have to be close to the ground state. In fact, it is possible to have a local minimum of relatively high energy. Formally, we can define a local minimum to be a state where any single spin flip will result in a higher energy state.

Consider a gauged RBM with weights \mathbf{W} , with some local minimum $\mathbf{s} = \{\mathbf{v}, \mathbf{h}\}$. We can use $I(+1, \mathbf{v})$ and $J(+1, \mathbf{h})$ to fully describe this state. In other words, we describe this local minimum by the subset of spins flipped from the $+1$ ground state. Then the energy of the local minimum can be expressed as

$$E(\mathbf{s}) = \left(\sum_{I, J} W_{ij} + \sum_{I^c, J^c} W_{ij} \right) - \left(\sum_{I, J^c} W_{ij} + \sum_{I^c, J} W_{ij} \right).$$

Note that this energy cannot decrease if we were to perform any single spin flip, then it can be shown that the following conditions must be satisfied

$$\begin{aligned} \sum_J W_{ij} &\geq \sum_{J^c} W_{ij} \quad \forall i \in I, & \sum_{J^c} W_{ij} &\geq \sum_J W_{ij} \quad \forall i \in I^c, \\ \sum_I W_{ij} &\geq \sum_{I^c} W_{ij} \quad \forall j \in J, & \sum_{I^c} W_{ij} &\geq \sum_I W_{ij} \quad \forall j \in J^c. \end{aligned} \quad (7)$$

In simpler terms, this basically means that for any local minimum, the sum of the weight elements of any row or column must be positive. Note that this is a necessary condition for the positive-sum condition but not a sufficient condition, which makes sense because a local minimum is not necessarily a global one.

IV. RANDOM FRUSTRATED-LOOP ALGORITHM

The frustrated-loop algorithm in its original form was proposed to generate spin-glass problems with known solutions to test the performance of the D-Wave quantum annealer [9]. Although the algorithm was initially proposed to be implemented on a 3D Ising model, it can be easily generalized to any graph that is not acyclic [11]. For the purpose of this paper, we focus on the case of a complete bipartite graph [11], which, as shown in Section II-B, is general enough to represent any graph structure.

Due to the non-local connectivity of a complete bipartite graph, the algorithm in its original form is unable to generate

sufficiently hard instances at high loop densities (see Section IV-J), so we propose a modified version of this algorithm (see Section V) that will be more suitable for the generating hard instances on a complete bipartite graph. Before doing that, however, we need to define a few concepts and recall how the original frustrated-loop algorithm is implemented [9].

A. Cycle

In the language of graph theory, a “loop” is simply a closed path on a graph with non-repeating edges or vertices (a cycle) [11]. For the case of an RBM, we try to construct a random cycle of a given length $2l$ on a bipartite graph. We start from a random visible node v_{i_1} , then “walk” to a random hidden node h_{j_1} , then return to the visible layer on another random visible node v_{i_2} , and so on. Note that for every iteration, the node selected must not be already within the path, until the very last iteration where we return from h_{j_l} back to v_{i_1} to “close the loop”. This cycle can be compactly expressed as

$$i_1 - j_1 - i_2 - j_2 - \dots - i_l - j_l - i_1.$$

From an algorithmic standpoint, this is fairly straightforward because we can simply select l nodes from the visible layer (where order matters) and l nodes from the hidden layer and connect them based on the order that they are chosen. Note that each edge within the cycle corresponds to a weight in the RBM energy since it denotes a two-body interaction between some visible spin and a hidden spin.

B. Frustrated Loop

We provide here a brief discussion of the random frustrated-loop algorithm in its original form [9]. The purpose of the algorithm is to generate an RBM instance with the ground state being $\mathbf{s} = +\mathbf{1}$. Trivially, one can set all the weights to positive. However, as discussed previously, this will result in an instance with zero frustration, or a ferromagnetic instance [21], and it will be extremely easy to solve. To make the instance non-trivial, we have to intentionally introduce negative weights in such a way such the ground state configuration $+\mathbf{1}$ is kept invariant. If the $+\mathbf{1}$ is no longer the ground state, then we have effectively lost track of the planted solution of the instance.

We then first begin by generating a loop of length $2l$ and set all the weights corresponding to the edges in the loop to $+1$ except for a single weight which we set to -1 . Then the energy of the $+\mathbf{1}$ state within this RBM subsystem is simply $E = -(2l - 1) + 1 = -2(l - 1)$. In other words, in this subsystem, we have to make at least one edge unsatisfied (or “break” one edge). It can be easily shown that there are multiple states with this energy (hence frustrated), corresponding to the different choices of edge to break in this loop. Therefore, the $+\mathbf{1}$ state is one of the degenerate ground states in this loop subgraph.

Now, we simply have to generate multiple loops with their weights set to $+1$ or -1 and “sum” them together. In other words, when multiple loops “intersect” at an edge, or when an edge is shared by multiple loops, we simply sum the weight contributions from the multiple loops at that given edge. And if an edge is not a part of any loop, then we set the corresponding

weight to 0. It can be shown that this procedure keeps the ground state $+\mathbf{1}$ invariant [9].

It is difficult to control the frustration index of instances generated by the original frustrated loop algorithm, because there is no parameter to directly control the frustration index. The frustration index is instead random and correlated with other parameters. To make direct and independent frustration control possible, we make three improvements on the original algorithm. First, since the frustration contribution from a frustrated loop is dependent on its length, we fix the loop length to be the smallest possible value, so that the frustration contribution of a single loop is fixed (see Section IV-C). Second, we allow the user to control the magnitude of the negative weight in the loop, which enables direct tunability of the frustration index (see Section IV-D). Lastly, we do not allow the negative weights to overlap with positive weights, so that the frustration index do not decrease with increasing loop density (see Section IV-E).

C. Loop Atom

In the original algorithm, only loops above a certain length are kept [9], because it has been argued that small loops may lead to excessively difficult instances [9]. The reason for this is because smaller loops have larger frustration indexes. However, in our random loop algorithm, it is possible to compensate for this large frustration index by “tuning down” the frustration through decreasing the magnitude of the negative weight in the loop (see Section IV-D). Therefore, the concern of having excessively difficult instances is inconsequential to us, and we can focus on generating the instances using the smallest loops possible.

The smallest simple cycle [11] that can be formed on a bipartite graph is of length 4. From now on, we refer such loop as a *loop atom*. From Eq. (6), it is obvious that the frustration index of a loop of length $2l$ to be

$$f = \frac{1}{2} \left(1 - \frac{2(l-1)}{2l} \right) = \frac{1}{2l},$$

so the frustration index is just the reciprocal of the length of the loop, with the loop atom having the maximum frustration 0.25. Therefore, we see that besides the algorithmic simplicity and computational efficiency of using loop atoms for instance generation, the loop atoms also allow for a wider range of frustration in the generated instances, meaning that they are more general than loops of other lengths.

In fact, it can be shown that a loop of any length can be decomposed as sum of loop atoms. Furthermore, it is even possible that the loop atoms are sufficiently general such that any gauged RBM instance with $f \leq 0.25$ can be decomposed as a conical combination [39] of loop atoms (see Section IV-F). To show that the former is true, it is sufficient to show that a loop of length $2l$ can be expressed as a sum of a loop of length $2(l-1)$ and a loop atom (by mathematical induction).

Let the loop that we wish to decompose be $i_1 - j_1 - \dots - j_l - i_1$. Without loss of generality, let us assume that all the weights in the loop are set to $+1$ except for the weight corresponding to the last edge $j_l - i_1$, which is set to -1 . Now, let a smaller loop of length $2(l-1)$ be $i_1 - j_1 - \dots - j_{l-1} - i_1$, with the

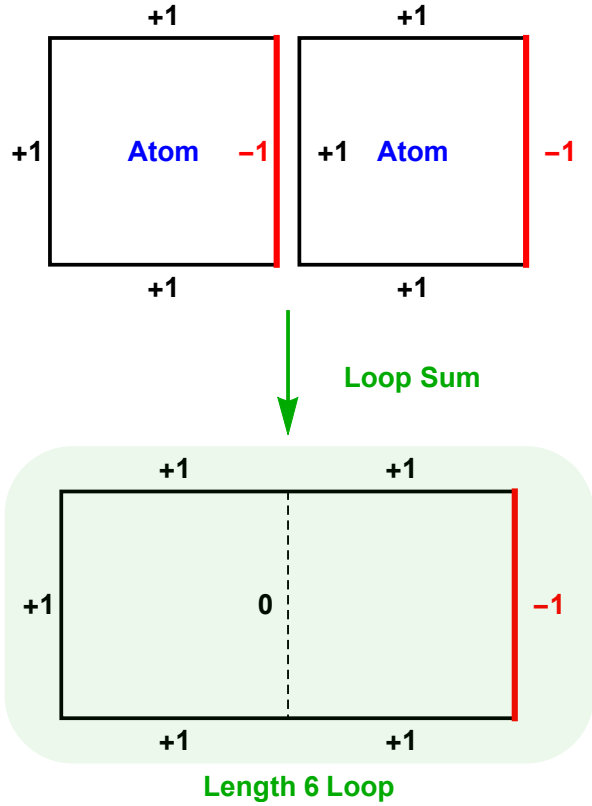


Fig. 3: Summing two-loop atoms results in a larger frustrated loop of length six. Note that the frustrated edge from the left loop and the positive edge from the right loop cancel out.

edge $j_{l-1} - i_1$ set to -1 . In addition, let the loop atom be $i_1 - j_{l-1} - i_l - j_l - i_1$ with the edge $j_l - i_1$ set to -1 . Note that the two loops intersect at $i_1 - j_{l-1}$. If we sum the smaller loop and the loop atom together, the weight contributions at the edge $j_{l-1} - i_1$ will cancel out, and we have formed a new loop $i_1 - j_1 - \dots - j_l - i_1$ with the edge $j_1 - i_1$ being -1 , which is simply the original loop that we wished to decompose.

Note that the action of us taking the “summation” of two frustrated loops is similar to the symmetric difference [28] operation of two cycles in graph theory, where we form a new cycle from two cycles by removing their common edges. However, the difference here is that a negative edge from one loop has to overlap with a positive edge from the other loop in order for the two edges to “cancel”. For the rest of the paper, when we refer to the *loop algorithm*, we only consider generating RBM instances with loop atoms.

D. Tunable Frustration

Recall that the frustration index of a single loop atom is 0.25. This gives rise to excessively difficult instances with a fixed frustration index. To allow for direct tunability of the frustration index for generating instances of variable difficulty, we then have to relax the condition that a loop atom must contain three $+1$ edges and one -1 edge. Instead, we only require the loop atom to satisfy the “positive-sum condition”, or simply ensuring that the sum of the weights of any two

edges be positive, corresponding to the 6 possible switching subsets in the 2×2 weight matrix of the loop atom subsystem. If we let the negative weight edge be $-\alpha$, then it can be easily shown that the “positive-sum” condition is equivalent to

$$1 - \alpha \geq 0,$$

or $\alpha \leq 1$. And since a frustrated loop must contain a frustrated edge by definition, we require that the negative weight $-\alpha$ be non-positive, so we have $0 \leq \alpha \leq 1$. Then, from Eq. (6), we see that the frustration contribution from a single loop can be expressed as

$$f = \frac{\alpha}{3 + \alpha},$$

with f ranging from 0 to 0.25. It should be noted that an instance generated with N loop atoms of a given α value will have a ground state energy of $-N(3 - \alpha)$, which can then be used to verify the correctness of the lowest energy that a solver finds.

E. Intersection

Often times, two or more loops will “intersect”, meaning that they will share one or more edges. They can either intersect constructively, meaning that all the weight contributions at the intersection edge are of the same sign, or intersect destructively, meaning that not all weight contributions are of the same sign. If we only focus on loop atoms with negative weights -1 , then we see that each loop contributes $-(1+1+1-1) = -2$ units of energy to the total energy of the RBM, and if we denote the total number of loops as N , then the ground state energy of the generated instance is simply $-2N$. Therefore, the expression for the frustration index in Eq. (6) can be reduced to

$$f = \frac{1}{2} - \frac{N}{\sum |W|}.$$

Note that if none of the loops intersect or if the loops only intersect constructively, then the absolute value of the total energy is just the sum of the absolute values of the weight contributions, which is 4 units of energy per loop, or $4N$ in total. This gives us a frustration index of $f = 0.25$, or the maximum frustration that the generated instances can have.

Even though constructive intersections do not affect the frustration index, destructive intersections, however, can decrease the frustration index. From this point on, when we use the term “intersection”, we refer solely to destructive intersection since it is the only non-trivial form of intersection with regards to the frustration index. To investigate exactly how destructive intersections affect the frustration index, we define an “intersection event” to be an event whenever at any edge, the weight contribution from the new loop has an opposite sign from the sign of the existing weight value.

For simplicity, we assume an unbiased $n \times n$ RBM. If we let k_1 be the total number of -1 contributions at a given edge, and k_2 be the total number of $+1$ contributions, then it is easy to see that the number of intersection events is $\min\{k_1, k_2\}$. Since every intersection event has a -2 contribution to $\sum |W|$,

if we let the total number of intersection events be N_\times , then the frustration index can be written as

$$f = \frac{1}{2} \left(1 - \frac{N}{2N - N_\times} \right) = \frac{1}{2} \left(1 - \frac{\frac{N}{n^2}}{2\frac{N}{n^2} - \frac{N_\times}{n^2}} \right)$$

where $\frac{N_\times}{n^2}$ is simply the average number of intersections per edge, with the total number of edges in an unbiased $n \times n$ RBM being n^2 . $\frac{N}{n^2}$ can be interpreted as the number of frustrated loops normalized by the system size. Note that the frustrated loop algorithm is symmetric with respect to any permutation of the edge labels, so the expected value of the average number of intersections per edge is the same as the that of any given edge, which we can denote as $\mathbf{E}(n_\times)$.

It can be shown that the intersection event at a given edge can be approximated as a Poisson process [40], and the number of intersections follows a complicated probability distribution only dependent on the quantity $\lambda = \frac{N}{n^2}$, and approaches a Poisson distribution with mean λ in the limit of large λ (see Appendix D). In other words, the expected value of the number of intersections per edge $\mathbf{E}(n_\times)$ starts from 0 and approaches $\frac{N}{n^2}$ asymptotically from below as N increases. If we were to approximate the expected value of the frustration index as

$$\mathbf{E}(f) = \frac{1}{2} \left(1 - \frac{\frac{N}{n^2}}{2\frac{N}{n^2} - \mathbf{E}(n_\times)} \right)$$

then it is clear that $\mathbf{E}(f)$ is only a function of $\frac{N}{n^2}$, since $\mathbf{E}(n_\times)$ itself is only dependent on $\frac{N}{n^2}$.

The frustration index f is $1/4$ initially and approaches 0 as N increases. This makes sense intuitively because as the number of loops increases, all the negative contributions are going to be dominated by the positive contributions at every edge, resulting in the trivial instance where all weight elements are positive, hence zero frustration. The main point here is that the frustration index is a random variable that is inversely correlated with the number of loops. Therefore, to minimize the difficulty decay associated with the increase in the number of loops and to remove random fluctuations in the frustration index, it is necessary that we prohibit the frustrated loops from intersecting destructively, and only allow constructive intersections to occur.

F. Generality

An interesting point briefly discussed in Section IV-C is the possibility of generating every possible RBM instance of $f \leq 0.25$ with only loop atoms. Before we extend on this discussion, we first point out that for any RBM instance, we can trivially superpose a ferromagnetic instance whose ground state is the same as that of the original system (which can be expressed in terms of a gauged weight matrix with all its elements being non-negative), and the sum of the original instance and the ferromagnetic instance will leave the ground state invariant. In other words, the sum of a gauged RBM weight matrix and another non-negative matrix results in another gauged RBM weight matrix.

This begs the question of whether any arbitrary gauged RBM matrix with $f \leq 0.25$ can be expressed as a conical combination of loop atoms and a non-negative matrix. A

conical combination is essentially a linear combination with all the coefficients being non-negative [39], where the non-negative coefficient condition is crucial here because we cannot “negate” the sign of a loop atom (such that we have three -1 edges and one 1 edge) as it will not leave the $+1$ ground state invariant.

The statement of this problem can be made more concise if we were to consider the weight matrix \mathbf{w} of an unbiased $n \times m$ RBM to be a vector in a nm dimensional vector space. A loop atom \mathbf{l}_c can also be considered a vector in the same vector space, with most of its components being zero. Note that there are $k = 4 \binom{n}{2} \binom{m}{2}$ possible loop atoms. Then the statement of the problem becomes whether we can find a set of k non-negative numbers $\{x_1, x_2, \dots, x_k\}$ such that the following is true

$$\sum_{c=1}^k x_c \mathbf{l}_c \leq \mathbf{w},$$

where the less than or equal sign implies that \mathbf{w} and the generated matrix can only differ by some non-negative vector (corresponding to the non-negative weight matrix of the superposed ferromagnetic instance). If we define a $nm \times k$ matrix to be $\mathbf{L} = [\mathbf{l}_1, \mathbf{l}_2, \dots, \mathbf{l}_k]$, then the statement can be made even more concise

Does the system $\mathbf{L}\mathbf{x} \leq \mathbf{w}$ have a solution with $\mathbf{x} \geq 0$? (8)

This is a system of inequalities, and this can be transformed into the following problem according to Farkas’ lemma [41]

Does the system $\mathbf{L}^T \mathbf{y} \geq 0$ have a solution with $\mathbf{w}^T \mathbf{y} < 0$ and $\mathbf{y} \geq 0$? (9)

Farkas’ lemma states that of the two statements (8) and (9) above, exactly one of them can be true at the same time. So proving statement (8) to be true is equivalent to proving that statement (9) is false (or proving that the negation of statement (9) is true). In Appendix F, we explicitly show that statement (9) is false for a 2×3 RBM. The result can be easily generalized to a $2 \times m$ RBM. However, the question of whether this still holds for a general $n \times m$ RBM is still open.

G. Biases

Recall in Section II-D, we showed that any bias term can be expressed as an interaction between a spin and some fixed spin v_{n+1} or h_{m+1} . In the previous sections, since we were limiting our discussion to only unbiased RBM, a frustrated loop does not contain any fixed spins, and all the spins within the loop can be freely flipped. However, for generating a biased RBM instance, it is possible for the loop to contain one or both of the fixed spins.

We first look at the case where the loop contains one fixed spin, and WLOG, we can assume the fixed spin to be h_{m+1} , then we can express the loop atom as $i_1 - j_1 - i_2 - (m+1) - i_1$. The two visible biases generated by this loop is $W_{i_1, m+1}$ and $W_{i_2, m+1}$ corresponding to the two edges connecting to h_{m+1} . At first glance, the fact that the spin h_{m+1} has to be kept fixed appears to imply that the column $m+1$ cannot be used to generate the switching subset directly, so the “positive-sum”

condition can be somewhat relaxed. However, this observation is not true as the elements in column h_{m+1} can in fact be flipped indirectly by flipping the elements in rows i_1 and i_2 followed by flipping the elements in column j_1 . Therefore, we see that the number of possible switching subsets of the loop is still 6, and the restrictions on the weight assignments of the loop will not change (see Section IV-D).

For a loop atom that contains both fixed spins, we can express the loop atom as $i_1 - (m + 1) - (n + 1) - j_1 - i_1$, which generates the visible bias $W_{i_1, m+1}$ and the hidden bias W_{n+1, j_1} . Note that the element $W_{n+1, m+1}$ denotes a constant offset that is independent of the spin configuration and can be thus disregarded. In this scenario, the elements in row $n + 1$ or column $m + 1$ cannot be flipped, so the switching subset can only be generated by row i_1 , column j_1 , or the combination of both. This gives rise to only 3 possible switching subsets in the loop atom subsystem, and a possible weight assignment that satisfies the ‘‘positive-sum condition’’ can be $W_{i_1, m+1} = W_{n+1, j_1} = 1$ and $W_{i_1, j_1} = -\alpha$ for $0 \leq \alpha \leq 1$. Note that in this case, the maximum frustration contribution from this loop atom (ignoring the weight $W_{n+1, m+1}$) is

$$f_{max} = \max_{\alpha} \frac{\alpha}{1 + 1 + \alpha} = \frac{1}{3}$$

which is greater than the 0.25 frustration contribution from a loop atom without any fixed spins. Therefore, we see that this higher frustration contribution can be exploited to generate instances with greater variation in difficulty.

H. Extension to General Graphs

Our choice to study the frustrated-loop algorithm on a bipartite graph is due to its simple structure for ease of theoretical analysis. However, if only a quick algorithmic implementation is of interest, then the frustrated-loop algorithm can be easily applied to any connected graph that is not a tree (or graphs with no cycles) [11]. One simply has to detect a sufficient number of random cycles on the graph, and generate a frustrated loop on each cycle by setting one of its edges to -1 and the rest to $+1$.

There exists an efficient way for finding all the cycles in a graph. We first begin by finding a cycle basis of the graph, or the minimal set of cycles from which all cycles can be generated through the symmetric difference operation [28]. The standard way to find a cycle basis is from the spanning tree of the graph, and many refined algorithms exist for this purpose [42]–[45]. After finding the cycle basis, we then take the symmetric difference between two or more randomly selected basis cycles to generate a new random cycle [46].

Recall that a cycle on a bipartite graph must contain an even number of edges. This is, however, not true for a general graph where the length of a simple cycle can be any integer greater than 2. In other words, a general graph may contain cycles of odd length, and the shortest cycle is of length 3. In the context of the frustrated loop, a length-3 loop gives rise to a frustration index of $\frac{1}{3}$ (in contrast to the maximal frustration of $\frac{1}{4}$ for a bipartite graph), meaning that it is possible to generate

instances of even higher frustration on a general graph than on a bipartite graph.

In terms of machine learning, this means that the frustrated loop algorithm can be applied to a variety of neural network structures. For example, this can be applied to a deep neural network [47] which can be described as a k -partite graph, or a fully connected Boltzmann machine that can be described by a complete graph [48].

I. Algorithm

A simple version of the frustrated-loop algorithm pseudocode is given in Algorithm 1, and a MATLAB implementation of the algorithm is available as the script `loop_rand.m` in the Github repository [25]. The code allows for the basic functionality of independent tuning of the frustration index and the loop density. As reasoned in Section IV-B, this algorithm prohibits destructive interference events and only uses loop atoms with the negative weight of the loop being tunable.

Note that variations on the code can be made, depending on the purpose of the test. Some examples are: the edge weights can be made normal random variables with small standard deviations to introduce more randomness; constructive interference can be also prohibited to have more consistent testing results; the bias terms can be intentionally made larger to generate more difficult instances. We only show the basic version here to avoid unnecessary complications.

Algorithm 1 Random Frustrated-Loop Algorithm

- 1: Generate an empty $(n + 1) \times (m + 1)$ matrix \mathbf{W}
 - 2: $n_loops = \lceil (n + 1) \times (m + 1) \times loop_density \rceil$
 - 3: $\alpha = \frac{3f}{1-f}$
 - 4: **for** $iter \in \llbracket [1, N_{loops}] \rrbracket$ **do**
 - 5: Choose a random column j_1
 - 6: Choose two random rows i_1, i_2 such that
 $W_{i_1 j_1} \geq 0 \wedge W_{i_2 j_1} \leq 0$
 - 7: Choose another random column j_2 such that
 $W_{i_1 j_2} \geq 0 \wedge W_{i_2 j_2} \geq 0$
 - 8: $W_{i_1 j_1} \leftarrow W_{i_1 j_1} + 1, W_{i_2 j_1} \leftarrow W_{i_2 j_1} - \alpha$
 - 9: $W_{i_1 j_2} \leftarrow W_{i_1 j_2} + 1, W_{i_2 j_2} \leftarrow W_{i_2 j_2} + 1$
 - 10: Generate a random state vector $\mathbf{s} \in \{-1, 1\}^{n+m}$
 - 11: Gauge \mathbf{W} such that \mathbf{s} is the lowest energy state
-

J. Limitation

Even though the frustrated-loop algorithm is able to generate maximally frustrated instances, this does not necessarily imply that the instances are sufficiently hard. This is due to the random nature of the distribution of the negative weights, making it incredibly difficult to give rise to a weight structure favorable for the population of closely spaced excited states and local minima. To be more specific, the expected value of each weight element for a maximally frustrated instance generated using the frustrated loop algorithm is $1/2$ with standard deviation of $\sqrt{3}/2$, and if we were to find the sum of a large subset of weights, the sum is $\frac{1}{2}|F| \pm \frac{\sqrt{3}}{2}\sqrt{|F|}$, and this

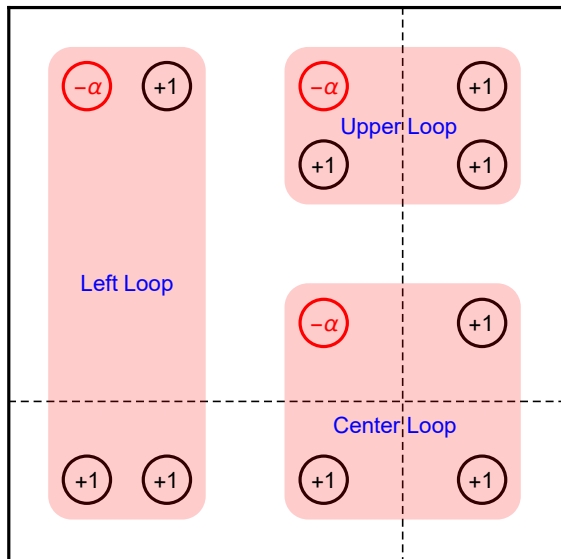


Fig. 4: The weight matrix is divided into four blocks by horizontal and vertical dashed lines. A left loop is on the left of the vertical line and crosses the horizontal line. An upper loop is above the horizontal line and crosses the vertical line. A center loop crosses the intersection of the two lines. Note that the negative weights are all located at the upper left block of the matrix.

value is most likely positive for a large $|F|$, since the relative standard deviation scales inversely with the size of the subset.

This problem is aggravated by the high connectivity of the RBM, where flipping even a few spins is equivalent to flipping a large number of weight elements, so flipping a cluster of spins will imply a large energy change. This makes it extremely difficult to support states that are close in energy but differ greatly in spins. Furthermore, the sum of the elements in any row or column is most likely positive, meaning that it is able to “guide” any single-spin update Markov-chain Monte Carlo (MCMC) algorithm to the ground state. This implies a huge difficulty for local minima to populate the energy landscape (see the Appendix G for a more formal discussion on the absence of local minima in large generated instances). Therefore, to generate sufficiently hard instances, we have to introduce some form of weight structure into the RBM, so that we have a greater population of local minima and closely spaced excited states.

V. STRUCTURED FRUSTRATED-LOOP ALGORITHM

As mentioned in Section IV-J, to generate sufficiently difficult instances at high loop density, the geometry and distribution of the loop atoms cannot be completely random, otherwise local minima and excited states cannot populate the energy landscape. Therefore, we must enforce certain structures on the loop atoms to make difficult instances at high loop density possible.

Algorithm 2 Structured Frustrated-Loop Algorithm

- 1: Generate an empty $(n + 1) \times (m + 1)$ matrix \mathbf{W}
- 2: $n_loops = \lceil (n + 1) \times (m + 1) \times loop_density \rceil$
- 3: $\alpha = \frac{3f}{1-f}$
- 4: $n_1 = n_2 = n_3 = \lceil \frac{N_{loops}}{3} \rceil$
- 5: **for** $iter \in \llbracket 1, n_1 \rrbracket$ **do**
- 6: Choose a random row i_1 in $\llbracket 1, \lceil \frac{n}{2} \rceil \rrbracket$;
- 7: choose a random row i_2 in $\llbracket \lceil \frac{n}{2} \rceil + 1, n \rrbracket$;
- 8: choose two random columns j_1, j_2 in $\llbracket 1, m \rrbracket$
- 9: such that:
- 10: $W_{i_1 j_1} \leq 0$, and $W_{i_1 j_2}, W_{i_2 j_1}, W_{i_2 j_2} \geq 0$
- 11: $W_{i_1 j_1} \leftarrow W_{i_1 j_1} - \alpha$, $W_{i_2 j_1} \leftarrow W_{i_2 j_1} + 1$
- 12: $W_{i_1 j_2} \leftarrow W_{i_1 j_2} + 1$, $W_{i_2 j_2} \leftarrow W_{i_2 j_2} + 1$
- 13: **for** $iter \in \llbracket 1, n_2 \rrbracket$ **do**
- 14: Choose two random rows i_1, i_2 in $\llbracket 1, n \rrbracket$;
- 15: choose a random column j_1 in $\llbracket 1, \lceil \frac{m}{2} \rceil \rrbracket$;
- 16: choose a random column j_2 in $\llbracket \lceil \frac{m}{2} \rceil + 1, m \rrbracket$
- 17: such that:
- 18: ...
- 19: **for** $iter \in \llbracket 1, n_3 \rrbracket$ **do**
- 20: Choose a random row i_1 in $\llbracket 1, \lceil \frac{n}{2} \rceil \rrbracket$;
- 21: choose a random row i_2 in $\llbracket \lceil \frac{n}{2} \rceil + 1, n \rrbracket$;
- 22: choose a random column j_1 in $\llbracket 1, \lceil \frac{m}{2} \rceil \rrbracket$;
- 23: choose a random column j_2 in $\llbracket \lceil \frac{m}{2} \rceil + 1, m \rrbracket$
- 24: such that:
- 25: ...
- 26: Generate a random state vector $\mathbf{s} \in \{-1, 1\}^{n+m}$
- 27: Gauge \mathbf{W} such that \mathbf{s} is the lowest energy state

A. Algorithm

We first start by introducing the algorithm (see Algorithm 2), followed by an explanation of why this algorithm performs better than the random frustrated-loop algorithm. The MATLAB implementation of this algorithm is available as the script `loop_struct.m` in the Github repository [25]. For the sake of consistency, we do not allow the loops to intersect. We start by dividing the gauged RBM weight matrix into four blocks: the upper-left block B_1 , the upper-right block B_2 , the lower-left block B_3 , and the lower-right block B_4 . The four blocks should be as close to having the same dimension as possible.

Note that a loop atom expressed in terms of a weight matrix can be visualized as four elements that form the vertices of a rectangle. To be more specific, the cycle $i_1 - j_1 - i_2 - j_2 - i_1$ can be expressed as a weight matrix with the indexes of its non-zero elements being (i_1, j_1) , (i_1, j_2) , (i_2, j_1) , and (i_2, j_2) , which obviously forms the shape of a rectangle represented in the 2D Cartesian coordinate. In this algorithm, we enforce the loops to have certain structures, such that the loops can be classified into one of the three kinds (see Figure 4):

- Left Loop: Two vertices of the loop atom must be in B_1 , and the other two vertices must be in B_3 .
- Upper Loop: Two vertices of the loop atom must be in B_1 , and the other two vertices must be in B_2 .
- Center Loop: Every block must contain a vertex of the loop atom.

Furthermore, we require that the vertex corresponding to the negative weight of the loop atom to be in B_1 . This effectively “concentrates” the negative weight elements into the upper left block, which, as we will see shortly, is favorable for generating difficult instances. Note that the choice of which block to concentrate the negative weights to is completely arbitrary, since a matrix can always be permuted such that the upper-left block becomes any of the four blocks, and it is even possible to “spread” the negative weights throughout the matrix through permutation.

B. Frustration and Local Minima

Here, we only consider loop atoms with three positive edge weights $+1$ and one negative edge weight $-\alpha$ with $0 \leq \alpha \leq 1$ (see Section IV-D). If we denote the number of left, upper, and center loops as N_1 , N_2 , and N_3 respectively, then it can be shown that

$$\begin{aligned} \sum B_1 &= (N_1 + N_2) - \alpha(N_1 + N_2 + N_3), \\ \sum B_2 &= 2N_2 + N_3 \quad \sum B_3 = 2N_1 + N_3, \quad \sum B_4 = N_3. \end{aligned}$$

If we choose $F = B_1 \cup B_4$ to be the switching subset, then the sum of all its elements is

$$\sum F = (1 - \alpha)(N_1 + N_2 + N_3).$$

We see that if $\alpha = 1$, then this sum is zero, meaning that there is at least a two-fold degenerate ground state. In fact, the spacing of the energy gap can be tuned by varying α . Note that any switching subset that is “close” to the state corresponding to F will also have small energy gaps from the ground state. In other words, the generated instance has highly degenerated low energy states (see Section III-D), which is an indication of a difficult instance.

In Appendix H, we demonstrate analytically that for sufficiently large number of center loops N_3 , there will also be a high population of local minima. In the next Section (Section VI), we show empirically, using simulated annealing, that there is an increase in difficulty for the structured frustrated-loop algorithm over the random frustrated loop algorithm in the regime of high loop density.

C. Extension to General Graphs

Just like how a loop atom can be expressed on an RBM weight matrix in terms of a rectangle with certain numbers on the vertices, a frustrated loop of length 4 can be expressed also as a rectangle on the adjacency matrix [11] of a general graph. To be more specific, the cycle $i_1 - i_2 - i_3 - i_4 - i_1$ can be expressed as a rectangle with indexes (i_1, i_2) , (i_2, i_3) , (i_3, i_4) , and (i_4, i_1) . Alternatively, since the graph is not necessarily bipartite so that the ordering of the indexes do not have to correspond to some the ordering of the two layers, the rectangle can also be (i_1, i_4) , (i_4, i_3) , (i_3, i_2) , and (i_2, i_1) , which is simply the “transpose” of the first rectangle. Therefore, to enforce the symmetric condition of the adjacency matrix, the loop can simply be expressed as the sum of the two rectangle representations.

Note that similar to the RBM case, we can, without loss of generality, force the element whose index corresponds to the top-left rectangle vertex to be negative, so that all the negative elements are “concentrated” at the top-left corner of the weight matrix. With this in mind, it is easy to check that the transpose of a left loop is simply an upper loop (with the negative element still being at the top-left), and the transpose of a center loop is still a center loop. Therefore, we see that we can choose to ignore, without loss of generality, the upper loop, and generate half of the adjacency matrix only with left and center loops, then take the sum of the generated matrix and its transpose to form the full adjacency matrix.

VI. TESTINGS

In this study, we focus on generating biased RBM instances of the form $n \times n$ (equal number of visible and hidden spins) using the random-loop algorithm (see algorithm 1) and the structured-loop algorithm (see algorithm 2). An RBM instance can be generated with three parameters: the size of the system n , the frustration index f (see Section IV-D), and the loop density ρ , where the loop density is defined as the ratio between the number of loops and the size of the system

$$\rho = \frac{N}{n}.$$

To study the difficulty of the generated instance, we use simulated annealing (SA) [49] as a powerful stochastic optimizer to solve the generated instances of different parameter triplets $\{n, f, \rho\}$, and we record the number of sweeps it takes for the solver to discover the ground state (see Section VI-A). The SA algorithm performs directly on the problem in the original RBM form (see Section II-C); for testing the performance of a general MAX-SAT solver, one can easily convert the problem into the corresponding MAX-2-SAT form. The conversion is available as the script `convert_to_SAT.m` in the Github repository [25].

The difficulty testings can be roughly divided into three parts. In the first two parts, we mainly study how the difficulty scales with $\{n, f, \rho\}$ with instances generated with the random-loop algorithm. In the first part, we study how the difficulty varies with the loop density, and observe the easy-hard-easy transitions, or hardness peaks [23], with the peak amplitudes and locations dependent on n . In the second part, we study how the difficulty scales with n for different frustration indexes f , and find that we can realize drastically different scaling behaviors for small changes in the frustration index, which is reminiscent of a *phase transition* [24] of spin-glass models. In the third part, we perform a comparative analysis between the random- and structured-loop algorithms in their abilities to generate difficult instances at high-loop density. For the structured-loop algorithm, we observe a second easy-hard transition beyond the first hardness peak, and also find a doubly-exponentially scaling difficulty improvement factor (over the random loop algorithm) with respect to the frustration index. All of the testing results can be easily reproduced by using the MATLAB script `main.m` which includes the functionality of generating instances with both the random and structured loop algorithm with user-defined parameters $\{n, f, \rho\}$.

A. Measurement of Difficulty

The difficulty of a generated instance is measured by the number of sweeps it takes for the simulated annealing (SA) algorithm (see Appendix I) to find the ground state configuration. A *sweep* is defined as an update over all the spins in the RBM. The SA solver is implemented in MATLAB with configurable inverse temperature β schedule, reinitialization schedule, and stopping criteria [49], which is available as the script `get_time_gibbs.m` under the GitHub repository [25]. For each generated instance, the solver is run on a single core of the AMD EPYC 7401 24-core processor. Since we are only interested in the scaling behavior instead of the actual computation time required to solve the instances, we choose the number of sweeps as a difficulty measure over the walltime to reduce timing inconsistencies caused by various unrelated factors such as CPU idle time [50], inefficiency of the interpretive language [51], and parallel efficiency [52]. If one wishes to obtain an estimate of the scaling behavior of the number of arithmetic operations required for SA to find the ground state, one can simply rescale the number of sweeps by a factor of n^2 [53], since the number of arithmetic operations required for a single SA iteration scales as $O(n^2)$ (see Appendix I).

The SA solver we implement uses a linearly increasing β schedule from 0.01 to $\log(n)$, such that the excited states are suppressed as $\frac{1}{n}$ [54]. The algorithm is run with some number of sweeps N_{sweep} before a reinitialization is performed if the ground state is not discovered. The algorithm terminates if the ground state is discovered, and the total number of sweeps N_{tot} summed over all the runs is recorded. For each instance, it would be ideal for us to use the optimal number of sweeps N_{sweep} per run such that the total number of sweeps N_{tot} is minimized to ensure that we are not overestimating the difficulty of the instance. If N_{sweep} is too small, then it is very unlikely for SA to discover the ground state in the highly non-convex energy landscape even if we were to perform many reinitializations, and if N_{sweep} is too large, then the rate of β may be unnecessarily slow for the given difficulty, meaning that the descent in RBM energy is unnecessarily “careful”, making the solver take longer than needed to find the ground state. The task of finding the optimal N_{sweep} is difficult, so to have a reasonable estimate of the optimal N_{sweep} for difficult instances, we first carefully tune N_{sweep} for easy instances (of small size n and small frustration f), and try to see how N_{sweep} scales with n and f , such that the optimal N_{sweep} can be extrapolated for larger n and f . More details of this method is given in Appendix J. In the script `main.m` [25], N_{sweep} is by default set to a value optimal for solving instances at the hardest loop density for every n and f (see Section VI-B and Section VI-C).

B. Difficulty vs. Loop Density

From our preliminary studies with small samples of generated instances, we find that the loop densities of the hardness peaks are rather insensitive to the frustration index or the sweep schedule. Therefore, we choose to perform this study with a frustration index of $f = 0.05$ so that the instances are

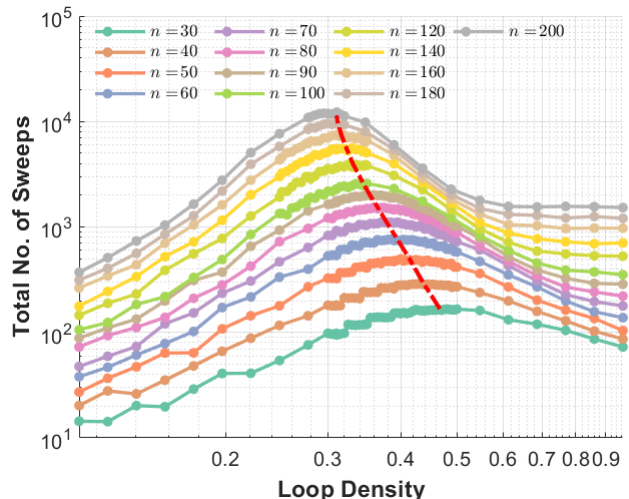


Fig. 5: Total number of sweeps, N_{tot} , versus loop density, ρ , plots for different values of system size, n . Note that the data points are more concentrated near the hardness peaks for higher resolution. Several plots for $n > 100$ are omitted in the Figure for visual clarity, but they are nonetheless used to perform the fitting. The dashed red line shows the exponential fitting $\rho(n)$ for the relationship between the loop density of the hardness peak and n , Eq. (10).

easy enough to be solved within a reasonable time window, meaning that we have the ability to solve a larger number of instances to reduce the uncertainty of our difficulty estimate. We choose to use a sweep schedule N_{sweep} that is optimized for solving instances of loop density $\rho = 0.47$ (see Appendix J), which is near the hardness peaks of small instances.

We try to locate the hardness peaks for instances of sizes ranging from $n = 30$ to $n = 200$ in increments of 10. For each size n , we perform a difficulty measurement for the following densities

$$\rho = 0.1 \times 1.12^k \quad k \in [[1, 20]],$$

which is a geometric series from 0.1 to around 1, meaning that the densities will appear evenly spaced out on a log scale. Measuring the difficulties over these densities will allow us to have a rough estimate of where the hardness peaks are located. For each size n , we then “zoom in” on the range of densities where we believe the hardness peak is within, and measure the difficulties over this range with a resolution of 0.005, which will allow us to pinpoint more precisely the location of the hardness peak.

In order to perform a difficulty measure for a given size of the system n and loop density ρ , we generate 10,000 different instances and solve them with SA to obtain a sample distribution of N_{tot} . We estimate the 95th percentile [55] of the distribution under the assumption that the distribution of N_{tot} is approximately log-normal [56] (see Appendix J), which we report as a difficulty measure.

The relationship between the difficulty and loop density for various n is shown in Figure 5. Note that for a larger system, the hardness peak is located at a smaller loop density. We

define the loop density of the hardness peak $\rho_{peak}(n)$ from which the generated instances will result in the highest 95th percentile of N_{tot} . We find that the relationship between the hardest loop density and n is well fitted by the following exponential decay function

$$\rho_{peak}(n) = 0.3035 + 0.2952 \times \exp(-0.0196n). \quad (10)$$

The explanation for the hardness peak is rather simple. When there are too few loops, the loops do not couple with each other and the system can be factored into subsystems contained within the individual loops. When there are too many loops, then it becomes very hard for local minima to populate the energy landscape (see Section IV-J). Note that unlike the original frustrated-loop algorithm used by the quantum annealing community [9], the loops in our algorithm are not allowed to intersect, so the decrease in difficulty cannot be attributed to the cancellation of frustration due to the overlap between a positive and negative weight (see Section IV-E).

We thus attribute the decrease in difficulty solely to the random nature of the distribution of the negative weights. Therefore, by using the structured-loop algorithm we present Section V, it is possible to retain the difficulty at high loop densities. An empirical study of this phenomenon will be presented in Section VI-D.

C. Difficulty vs. Frustration

After determining the hardest loop density $\rho(n)$ for each n , we now have the ability to generate the hardest instances for a given pair of $\{n, f\}$. This allows us to study the scaling behavior of the difficulty over the hardest instances with respect to n for different frustration indexes f . For this study, we use the following 8 frustration indexes

$$f = \{0.05, 0.10, 0.15, 0.2, 0.21, 0.22, 0.23, 0.24\}.$$

For each f , we choose a series of sizes n to measure the difficulty. Since the higher the frustration, the more difficult the instances, we can only use small n for highly frustrated instances to guarantee a solution within a reasonable time window.

For this study, we use a sweep schedule N_{sweep} that is optimized for solving the hardest instances (see Appendix J). The sample size of the instances for each pair of $\{n, f\}$ ranges from 100 to 10000 depending on how difficult the instances are (the harder the instances, the smaller the sample size). Since the 95th percentile estimate for N_{tot} is noise dominated for small sample size, we instead opt to use geometric mean as a measure of difficulty.

The results are shown in Figure 6, where the data points are fitted with either a polynomial or exponential function depending on the convergence of the fitting. The interesting result to note here is that by tuning the frustration index, we can achieve different scaling laws for the difficulty. In the regime of low frustration, or $f = \{0.05, 0.10, 0.15\}$, the scaling appears to be quadratic. For medium frustration, or $f = \{0.2, 0.21\}$, the scaling follows a sub-exponential trend of the form $Ae^{b\sqrt{n}}$.

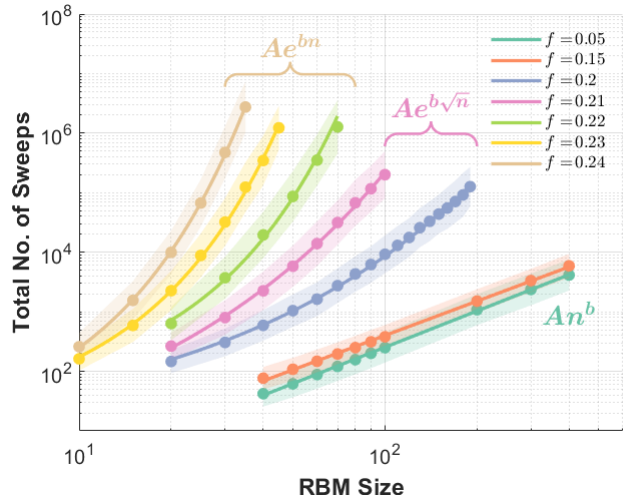


Fig. 6: Scaling behavior of the difficulty with respect to system size, n , for different frustration indexes, f . Note that the plots are on a log-log scale such that a polynomial scaling behavior will appear as a straight line, and an exponential scaling behavior will appear as a curve. The solid curves shown in the Figure are fitted curves for the estimated geometric mean of the N_{tot} samples. The shaded area denotes the deviation from the mean by 0.5 times the estimated standard deviation in log space, which corresponds to roughly the 31th to 69th percentile estimates assuming an underlying log-normal distribution. For $f = \{0.05, 0.1, 0.15\}$, the data points are well fitted by a polynomial function of the form Ab^n with parameters $\{A, b\} = \{0.0225, 2.0259\}$, $\{0.0284, 2.0168\}$, $\{0.0591, 1.9150\}$ respectively. For $f = \{0.2, 0.21\}$, the data are well fitted by an exponential function of the form $Ae^{b\sqrt{n}}$ with parameters $\{A, b\} = \{6.2343, 0.7227\}$, $\{1.0184, 1.2283\}$. For $f = \{0.22, 0.23, 0.24\}$, they are well fitted by an exponential function of the form Ae^{bn} with parameters $\{A, b\} = \{30.7289, 0.1579\}$, $\{13.3808, 0.2564\}$, $\{5.9172, 0.3738\}$

And for high frustration, or $f = \{0.22, 0.23, 0.24\}$, the scaling follows the standard exponential growth of the form Ae^{bn} .

The drastically different scaling laws that we can achieve by tuning f seems to hint at two separate discontinuous phase transitions in the difficulty scaling behavior driven by the frustration of the system. Whether this corresponds to an actual phase transition in the corresponding physical model is not entirely clear. Nevertheless, it is important to note that phase transitions in classical [24] or quantum spin-glass models [57] have been well-studied, and in the latter case, it is known that a *quantum* phase transition can be driven by the strength of the frustrated coupling terms [58]. However, we believe that there has been no prior studies on phase transitions in *classical* systems driven by the frustration index (as a continuously varying parameter). Therefore, this result has no direct theoretical analogue, and an explanation of why two separate phase transitions can be driven by the frustration index is not entirely obvious at the current stage of our work.

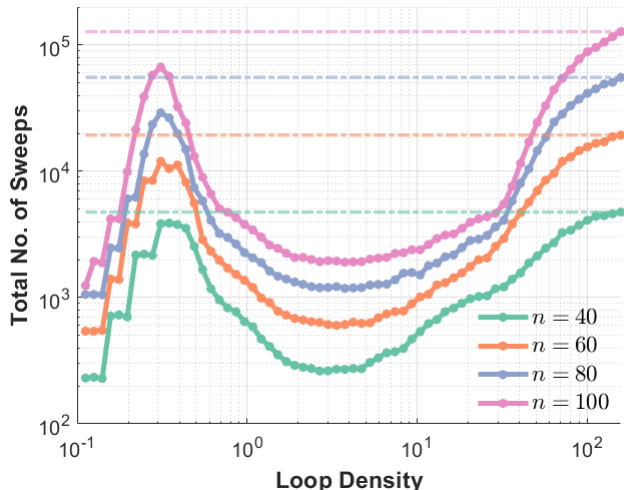


Fig. 7: Easy-hard-easy-hard transitions at four different system sizes, n . In addition to the expected hardness peaks at the low loop density regime (to the left), we see an additional increase in difficulty at the high loop density regime beyond the initial hardness peak for instances generated with the structured-loop algorithm.

D. Structured-Loop Algorithm

Note that so far, we have been looking only at systems with small loop density, meaning that a large percentage of the RBM weight matrix elements are zero. (For instance, if we take an unbiased 100×100 RBM of clause density $\rho = 0.47$, then the percentage of non-zero matrix elements is $\frac{\rho n}{n^2} = 4.7 \times 10^{-3}$.) However, to generate instances where the underlying graph is a more general complete bipartite graph, it is necessary for us to generate more connections between the spins, or have instances of higher loop density. In Section IV-J, we argued that in the regime of high loop density, the random loop algorithm is unable to generate sufficiently difficult instances due to a sparse population of local minima. In Section V, we introduced a modified version of the frustrated loop algorithm that addresses this issue, allowing for a greater population of local minima.

Here, we show empirically that the instances generated by the structured-loop algorithm exhibits a second easy-hard transition beyond the initial hardness peak (see Section VI-B). In other words, we observe an increase in difficulty as we approach the high loop density regime, which was not observed in the instances generated by the original version of the algorithm [9]. We compare the difficulty of the instances generated by the frustrated loop algorithm with that of the random loop algorithm and observe a constant factor of increase over all system sizes for a given frustration index. This factor of difficulty increase seems to scale super-exponentially (a scaling law of the form $e^{Ae^{bf}}$) with respect to the frustration index f .

To study the trend of the difficulty versus density relation of instances generated by the structured-loop algorithm, we focus on instances of sizes ranging from $n = 40$ to $n = 100$ in increments of 20 with the frustration index fixed at $f =$

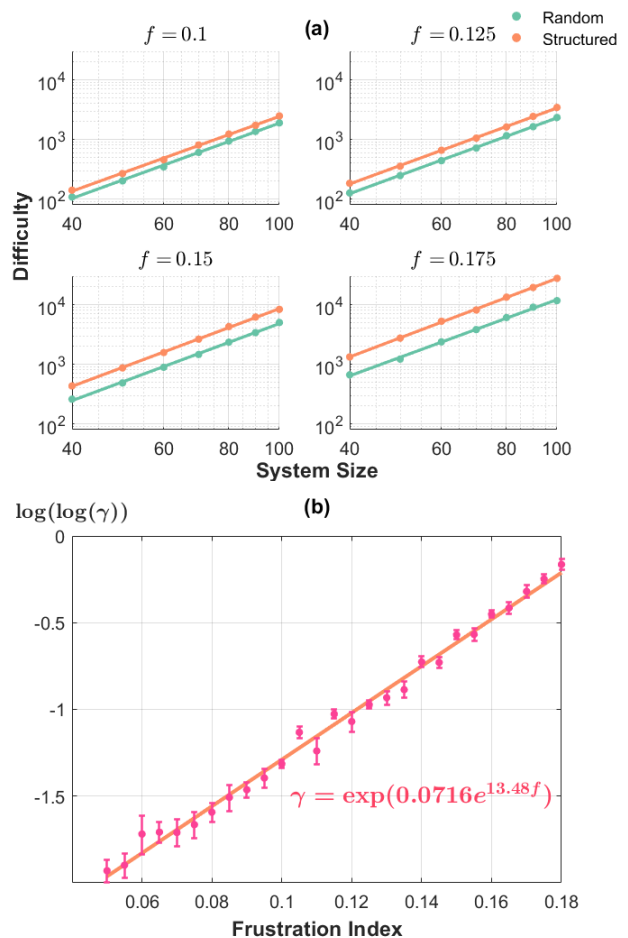


Fig. 8: (a) The difficulty scaling with respect to system size for instances generated with both the random- (green curves) and structured-loop (orange curves) algorithms of various frustration indexes, f . The data points are plotted on a log-log scale, and fitted with a polynomial function of the form An^b with a least-square fitting in log-space. Note that the power of the scaling does not vary considerably with the frustration index or the algorithm used, evident from the fact that the fitted lines form parallel lines with approximately the same slopes across the four frustration indexes. However, the gap between the two lines increases with increasing frustration index, meaning that the improvement factor is greater for instances generated at a higher frustration index. (b) Relationship between the improvement factor, γ , and the frustration index. The data points are fitted with a super-exponential function of the form $e^{Ae^{bf}}$, which is represented by a straight line if we take the double logarithm of the improvement factor axis (the y-axis). For each frustration index, the error bar represents the estimated standard deviation (in log-space) of the sample mean of γ values taken over all the system sizes.

0.2, and perform difficulty measurements over the following densities

$$\rho = 0.1 \times 1.12^k \quad k \in [[1, 65]]$$

with the maximum density being around $\rho_{max} \approx 158$. For each difficulty measurement, we take the 95th percentile of N_{tot} sampled from 10,000 separate instances. From Figure 7, we observe that the difficulty grows beyond the initial hardness peak for all four system sizes.

To see the improvement of the structured-loop algorithm over the random-loop algorithm for instances generated at different frustration indexes, we fix the loop density of the instances at $\rho = 100$ (high loop density), and study how the difficulty scales with the system for instances generated with both algorithms at the following frustration indexes

$$f = 0.05 + 0.005k, \quad k \in [[0, 26]], \quad (11)$$

or frustration indexes from 0.05 to 0.18 with increments of 0.005. The difficulty measurement is performed across system sizes from $n = 40$ to $n = 100$ in increments of 10, and the 95th percentile of N_{tot} sampled from 10,000 instances is used for each difficulty measurement.

The difficulty scaling behavior of the two algorithms for four selected frustration indexes are plotted in Figure 8. We observe that the scaling behavior of the two algorithms follows the same power law, though it is apparent that the scaling prefactor of the structured-loop algorithm is greater. To quantify the difficulty improvement of the structured-loop algorithm over the random-loop algorithm, we define the improvement factor γ as the ratio between the scaling prefactors of the structured- and random-loop algorithms. In other words, if we assume that the difficulty of the random-loop algorithm scales as $A_r e^{bn}$, and the structured-loop algorithm scales as $A_s e^{bn}$, then γ is defined as

$$\gamma = \frac{A_s}{A_r}.$$

Note that an estimate of γ can be obtained by performing a least-square fitting on the scaling behavior of the two algorithms in log-space with the constraint that the scaling coefficients b of the two algorithms must be the same for a given frustration index. Note that this procedure is equivalent to taking the geometric mean of the ratios between the difficulties of the structured- and random-loop algorithms over the list of system sizes.

From Figure 8(a), it can already be seen that γ increases with the frustration index. In Figure 8(b), the relationship between γ and f is plotted over all frustration indexes used in the study (see Eq. (11)), so the correlation between γ and f is better visualized. The relationship between γ and f is well fitted by a super-exponential function of the form $e^{Ae^{bn}}$, or the linear function $\log(A) + bn$ if we take the double logarithm of the difficulty. In other words, the structured-loop algorithm is super-exponentially more effective in improving the difficulties of instances generated at a higher frustration index.

In addition to showing the effectiveness of the structured loop algorithm, this super-exponential scaling behavior with respect to the frustration index, together with the phase transition behavior studied in Section VI-C, provides strong

empirical evidence of the fact that the frustration index is central in studying optimization problems of the weighted MAX-2-SAT form.

VII. CONNECTION TO RBM PRE-TRAINING

Our study is mainly focused on generating weighted MAX-2-SAT instances of tunable difficulty with frustrated loops, and the RBM terminology was mostly used so far as a convenient denotation for a general bipartite spin glass on which the instances are generated. Nevertheless, there are several substantial connections of this study to the field of machine learning, with some directly related to the pre-training of an RBM [12]. The connections to the pre-training of RBM mainly form two branches, one practical and one heuristic.

The practical application is that solving for the minimum RBM energy is equivalent to finding the mode of the RBM model distribution, which can be used to make highly informative weight updates during the pre-training, such that the model distribution is guaranteed to converge to a distribution that is close to the data distribution [20]. The number of iterations to convergence is also greatly reduced compared to standard pre-training methods such as contrastive divergence (CD) [59]. The heuristic connection is that the frustration index of the RBM contains a lot of information on the behavior of the RBM during pre-training, meaning that it is possible to use the frustration index as an important indicator for certain properties of the RBM (see Section VII-B). These connections will be studied in more depth both analytically and empirically in another work [20].

A. Pre-training Using the Mode

During pre-training, to minimize the Kullback-Leibler (KL) divergence between the data distribution and the model distribution, the weights should be updated according to the following rule [12]

$$\Delta W_{ij} = \mu(\langle v_i h_j \rangle_D - \langle v_i h_j \rangle_M),$$

where μ is some learning rate. The first term is the expected value of $v_i h_j$ over the *data distribution*, and the second term is the expected value over the *model distribution*. It can be shown that the weight update direction directly opposes the exact gradient of the KL divergence, meaning that the KL divergence is expected to decrease as we pre-train the RBM.

However, there are two main problems with this update. First, the KL divergence is (as any other loss function in machine learning) highly non-convex [60], meaning that following the gradient will likely lead to a local minimum instead of the global one. Second, even though the first term is easy to compute in an RBM, the second term is difficult since it requires summing over an exponential number of configurations [12]

$$\langle v_i h_j \rangle_M = \sum_{\mathbf{v}, \mathbf{h}} p(\mathbf{v}, \mathbf{h}) v_i h_j,$$

where the expression can be simplified by tracing out the hidden layers, but still leaving an exponential number of visible layer configurations. This term is usually approximated

using *contrastive divergence* [59], which is a form of Markov chain Monte Carlo (MCMC). It is well known that using contrastive divergence results in poor convergence and stability for the KL divergence [61].

The reason why CD performs poorly is because it is prone to being “frozen” under one of the modes in a multimodal distribution, and since it is energetically expensive to transition to another mode by performing single node flips, this essentially “traps” the Markov chain and prevents it from effectively exploring the entire probability measure [15]. One obvious solution is to reinitialize the Markov chain at the global mode whenever it is trapped, and this has in fact been shown to be effective in improving the mixing time of the Markov chain [17, 18]. Recently, we have discovered that the usefulness of the mode goes beyond the effective reinitialization for the MCMC, and we will discuss this aspect in another work [20].

B. Frustration Index as an Indicator

During RBM pre-training, the KL divergence [19] can be used as an indicator of how “close” the model and data distributions are, so that the pre-training process can be monitored. However, computing the KL divergence is usually impractical for large systems since it requires computing the partition function which involves an exponentially scaling number of sums, and current methods for the estimation of KL divergence are rather inaccurate [62].

Alternatively, the frustration index can be used as an indicator of how the model distribution is evolving. Note that during pre-training, the model distribution evolves to fit the data distribution, which is a distribution with multiple dominant modes far apart from each other [12]. This is equivalent to an RBM energy landscape with closely spaced energies near the ground state which differ by large number of node flips. In Section III-D, we argued that the existence of highly degenerate ground states is only possible in a highly frustrated system. Therefore, during pre-training, the frustration index must rise to a relatively large value, and if it does not, then it indicates the possibility of a pre-training instance that is not converging towards the data distribution. Note that computing the frustration index is computationally inexpensive once the minimum energy configuration is known [22], so the frustration calculation can be scheduled to occur in conjunction with the solution of the global mode.

In Figure 9, we plot the evolution of the frustration index as we pre-train a 9×6 RBM using the standard CD-1 gradient estimate [59], and we observe a clear increasing trend with the exception of a small dip in the middle of the pre-training iterations. The frustration index is initially zero, and grows until it plateaus to a value around 0.18, which is at the borderline where difficulty scaling behavior transits from polynomial to exponential (see Fig. 6). This implies that the effectiveness of training the RBM with the mode is at the computational expense of finding the mode in the first place during a pre-training iteration, which is as expected from “no free lunch” theorem of optimization algorithms [63], as the difficulty of minimizing the KL divergence is “transferred”

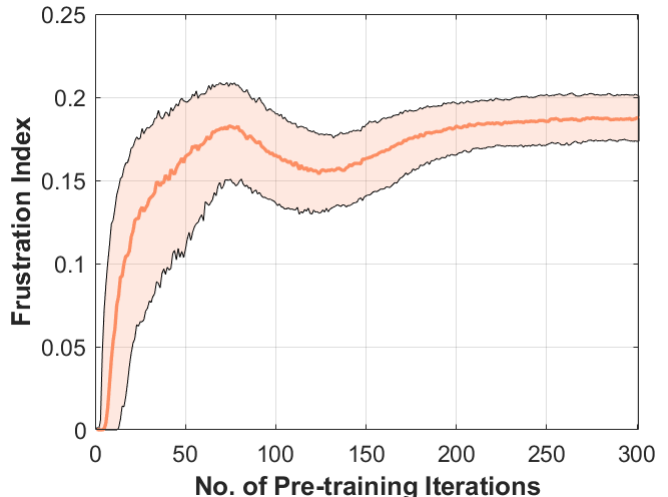


Fig. 9: The evolution of the frustration index in the pre-training iterations for 1000 different initial weight parameter assignments. The RBM size is 9×6 , and the data distribution consists of 9 visible layer configurations of equal weights generated by a shifting bar of length 5 [64]. The solid line shows the median of the frustration indexes obtained from the 1000 training instances at every iteration, and the shaded area is enclosed above by the estimated 80th percentile of the sample distribution and below by the 20th percentile of the sample distribution.

to the difficulty of finding the mode. Nevertheless, from a practical standpoint, if we were to use a highly effective MAX-SAT solver, the reduced number of iterations required for the KL divergence to converge below some desired set point may largely offset the computational expense for locating the global mode.

The goal of pre-training the RBM is commonly believed to serve the purpose of acquiring better initial weight values for the supervised learning stage when the data labels are scarce [65]. On the other hand, the goal of supervised learning is to increase the certainty of the output node activations such that they correspond to the data labels [47]. However, it was recently discovered that pre-training of an RBM is also capable of achieving a higher certainty of hidden node activations [66]. In a subsequent work [20], we will show that the increase in the certainty of hidden node activations is strongly correlated with the increase in the frustration index of the RBM. This correlation may be mediated by information compression, in the sense that the increase in hidden node activations is potentially related to the drift-diffusion transition on the information bottleneck (IB) curve [67], which itself may parallel the phase transition phenomenon driven by the frustration index (see Section VI-C) as the RBM is pre-trained. It will be interesting to explore these potentially useful directions of study even further to establish the connection between the frustration index and the dynamical properties of the RBM during unsupervised and supervised training.

VIII. CONCLUSION

In this paper, we reformulated the frustrated-loop algorithm, originally conceived to test quantum annealers, in such a way that it can be directly applied to generating weighted MAX-2-SAT instances of tunable difficulty. In addition, we introduced the structured-loop algorithm for the purpose of generating difficult instances at high loop density, and showed empirically a super-exponential scaling behavior of the difficulty improvement factor with respect to the frustration index. Another unexpected discovery is the possible two-stage phase transitions in the difficulty scaling behavior driven by the frustration index. We hope this result will motivate further theoretical work on studying spin-glass models from the perspective of the frustration index. On a more practical note, the structured-loop algorithm is able to efficiently generate general weighted MAX-2-SAT instances of tunable difficulty and of varying clause density, which can be used to effectively evaluate the performance of a wide class of solvers, particularly the state-of-the-art solvers participating in the most recent Max-SAT evaluations [68]. It would also be interesting to evaluate some other types of stochastic solvers, e.g., those based on cluster spin-flip updates [69, 70] and parallel tempering [71] with iso-energetic cluster moves [72]. We can also investigate the performance of unconventional solvers such as solvers that operate under continuous-time dynamics [73] or solvers based on the novel memcomputing paradigm [74, 75]. The latter employs memory-assisted dynamics to realize long-range order in the variable space, which allows the system to navigate the non-convex energy landscape corresponding to the optimization problem [76]. We leave these testings for future work.

IX. ACKNOWLEDGMENTS

H.M. acknowledges support from a DoD-SMART fellowship. M.D. acknowledges partial support from the Center for Memory and Recording Research at UCSD.

APPENDIX

A. Invariance of the Maximum in Bipartite Conversion

Let us assume that we have some assignment where $\mathbf{v}_1 \neq \mathbf{h}_1$ that maximizes the polynomial in Eq. (4). Let $\mathbf{v}_0 = \mathbf{h}_0$ be some random assignment. Then in order for $\{v_1, h_1\}$ to maximize the polynomial, it is necessary that

$$\begin{aligned} & \sum_{i=1}^n B_i v_{1i} + \sum_{i=1}^n \sum_{j>i}^n Q_{ij} v_{1i} h_{1j} + C(\mathbf{v}_1, \mathbf{h}_1) \\ & \geq \sum_{i=1}^n B_i v_{0i} + \sum_{i=1}^n \sum_{j>i}^n Q_{ij} v_{0i} h_{0j} + C(\mathbf{v}_0, \mathbf{h}_0), \end{aligned}$$

which implies that

$$\begin{aligned} & \sum_{i=1}^n B_i (v_{1i} - v_{0i}) + \sum_{i=1}^n \sum_{j>i}^n Q_{ij} (v_{1i} h_{1j} - v_{0i} v_{0j}) \\ & \geq C(\mathbf{v}_0, \mathbf{h}_0) - C(\mathbf{v}_1, \mathbf{h}_1) \\ & \geq \sum_{i=1}^n |B_i| + \sum_{i=1}^n \sum_{j>i}^n |Q_{ij}|, \end{aligned}$$

which is impossible. Therefore, the maximum must be an assignment where $\mathbf{v} = \mathbf{h}$, then the maximization problem reduces to the following

$$\begin{aligned} & \max_{\mathbf{v}, \mathbf{h}} \left\{ \sum_{i=1}^n B_i v_i + \sum_{i=1}^n \sum_{j>i}^n Q_{ij} v_i h_j + C(\mathbf{v}, \mathbf{h}) \right\} \\ & = \max_{\mathbf{v}=\mathbf{h}} \left\{ \sum_{i=1}^n B_i v_i + \sum_{i=1}^n \sum_{j>i}^n Q_{ij} v_i h_j \right\} \\ & = \max_{\mathbf{v}} \left\{ \sum_{i=1}^n B_i v_i + \sum_{i=1}^n \sum_{j>i}^n Q_{ij} v_i v_j \right\}, \end{aligned}$$

which is exactly the same problem of maximizing the original QUBO problem in Eq. (2).

B. Variance of Energy Gaps in RBM of Random Weights

Let us consider an RBM instance of independent and randomly distributed random weights. From Eq. (5), we have the following

$$\begin{aligned} & \text{Var}(E(\mathbf{s}') - E(\mathbf{s})) \\ & = \text{Var} \left[-2 \sum_{ij} W_{ij} v_i h_j \right] \\ & = 4 \text{Var} \left[\sum_{ij} W_{ij} v_i h_j \right] \\ & = 4 \left[\sum_{ij} \text{Var}(W_{ij} v_i h_j) + \sum_{i<i',j} \text{Cov}(W_{ij} v_i h_j, W_{i'j} v_{i'} h_j) \right. \\ & \quad \left. + \sum_{i,j<j'} \text{Cov}(W_{ij} v_i h_j, W_{ij'} v_i h_{j'}) \right. \\ & \quad \left. + \sum_{i<i',j<j'} \text{Cov}(W_{ij} v_i h_j, W_{i'j'} v_{i'} h_{j'}) \right], \end{aligned}$$

where $\{i, j\} \in F$ is assumed. The last covariance term is just zero since all the terms inside are independent. While the second term is

$$\begin{aligned} & \text{Cov}(W_{ij} v_i h_j, W_{i'j} v_{i'} h_j) \\ & = \mathbf{E}(W_{ij} v_i h_j W_{i'j} v_{i'} h_j) - \mathbf{E}(W_{ij} v_i h_j) \mathbf{E}(W_{i'j} v_{i'} h_j) \\ & = h_j^2 [\mathbf{E}(W_{ij} v_i W_{i'j} v_{i'}) - \mathbf{E}(W_{ij} v_i) \mathbf{E}(W_{i'j} v_{i'})] \\ & = 1 \times 0 = 0, \end{aligned}$$

where we used the fact that $h_j^2 = 1$ and $\mathbf{E}(W_{ij} v_i W_{i'j} v_{i'}) = \mathbf{E}(W_{ij} v_i) \mathbf{E}(W_{i'j} v_{i'})$. Similarly

$$\text{Cov}(W_{ij} v_i h_j, W_{ij'} v_i h_{j'}) = 0.$$

We then have:

$$\begin{aligned} & \text{Var}(E(\mathbf{s}') - E(\mathbf{s})) \\ & = 4 \sum_{ij} \text{Var}(W_{ij} v_i h_j) \\ & = 4|F| [\mathbf{E}(W_{ij}^2 v_i^2 h_j^2) - \mathbf{E}(W_{ij} v_i h_j)^2] \\ & = 4|F| \mathbf{E}(W_{ij}^2) \\ & = 4|F| (\mu^2 + \sigma^2), \end{aligned}$$

where we used the fact that $\mathbf{E}(W_{ij} v_i h_j) = 0$, and $\mathbf{E}(W_{ij}^2 v_i^2 h_j^2) = v_i^2 h_j^2 \mathbf{E}(W_{ij}^2) = \mathbf{E}(W_{ij}^2)$.

C. Metric Conditions

In this Section, we prove that the cardinality $|F(\mathbf{s}, \mathbf{s}')|$ satisfies the four conditions of a metric in the case of a biased RBM. Recall that $|F(\mathbf{s}, \mathbf{s}')| = n_v m + n m_h - 2n_v m_h$.

- *Non-negativity*: $|F| \geq 0$ trivially because the cardinality of a set must be positive.
- *Identity of indiscernibles*, or $|F(\mathbf{s}, \mathbf{s}')| = 0 \Leftrightarrow \mathbf{s} = \mathbf{s}'$: If $\mathbf{s} = \mathbf{s}'$, then $n_v = m_h = 0$, so $|F| = 0$. If $|F| = 0$, then $n_v m + n m_h - 2n_v m_h = 0$. The only non-trivial solution is $n_v = n$ and $m_h = m$, which is not possible for a biased RBM since it would imply all the spins (including the ghost spins) being flipped. Therefore, we recover the trivial solution $n_v = m_h = 0$, implying that $\mathbf{s} = \mathbf{s}'$.
- *Symmetry*, or $|F(\mathbf{s}, \mathbf{s}')| = |F(\mathbf{s}', \mathbf{s})|$: Since the same spins have to be flipped to make the transition $\mathbf{s} \rightarrow \mathbf{s}'$ and the reverse transition $\mathbf{s}' \rightarrow \mathbf{s}$, this implies $F(\mathbf{s}, \mathbf{s}') = F(\mathbf{s}', \mathbf{s})$, or $|F(\mathbf{s}, \mathbf{s}')| = |F(\mathbf{s}', \mathbf{s})|$.
- *Triangle Inequality*, or $|F(\mathbf{s}, \mathbf{s}'')| \leq |F(\mathbf{s}, \mathbf{s}')| + |F(\mathbf{s}', \mathbf{s}'')|$: Let $|F(\mathbf{s}, \mathbf{s}')| = n_v m + n m_h - 2n_v m_h$, $|F(\mathbf{s}', \mathbf{s}'')| = n'_v m + n m'_h - 2n'_v m'_h$, and $|F(\mathbf{s}, \mathbf{s}'')| = n''_v m + n m''_h - 2n''_v m''_h$. Note that $n_v + n'_v \geq n''_v$, because the total number of visible spins being flipped cannot be greater than the sum of the number of spins flipped during the two individual flipping stages. Similarly, $m_h + m'_h \geq m''_h$. Then $|F(\mathbf{s}, \mathbf{s}')| + |F(\mathbf{s}', \mathbf{s}'')| = (n_v + n'_v)m + n(m_h + m'_h) - 2(n_v m_h + n'_v m'_h) \geq (n_v + n'_v)m + n(m_h + m'_h) - 2(n_v + n'_v)(m_h + m'_h) \geq n''_v m + n m''_h - 2n''_v m''_h = |F(\mathbf{s}, \mathbf{s}'')|$.

D. Intersection Event

For the sake of generality, we ignore the topology of the graph for now, and simply denote the probability of a given edge to be a part of a randomly generated loop atom to be p . Of course, we have to assume symmetry of the connectivity and our algorithm to be unbiased such that the value of p is the same for all edges. This is obviously satisfied by a cubic lattice for $d \geq 2$ and also any bipartite graph with $n \geq 2$ and $m \geq 2$. Now, we can easily see that for any given edge, the probability that this edge receives a $+1$ contribution is $\frac{3}{4}p$, the probability that it receives a -1 contribution is $\frac{1}{4}p$, and the probability that it receives 0 contribution is $1 - p$. Therefore, if we denote the total number of random loop atoms as N , the number of -1 contributions on a given edge as k_1 , and the number of $+1$ contributions as k_2 , then $\{k_1, k_2\}$ follows a multinomial distribution

$$P(k_1, k_2) = \binom{N}{k_1, k_2} \left(\frac{1}{4}p\right)^{k_1} \left(\frac{3}{4}p\right)^{k_2} (1-p)^{n-k_1-k_2}.$$

The expected number of intersections on any edge is thus simply $\mathbf{E}(\min\{k_1, k_2\})$. Note that there are a few simplifications we can make to this problem. First, we can make the assumption that $p \ll 1$, which is true if the graph is large enough. If denote $\lambda = Np$, then the marginal distributions of k_1 and k_2 are Poisson distributions

$$P(k_1) = \frac{e^{-\lambda/4} (\lambda/4)^{k_1}}{k_1!}, \quad P(k_2) = \frac{e^{-3\lambda/4} (3\lambda/4)^{k_2}}{k_2!}.$$

Note that since $p \ll 1$, we can also make the approximation that these two random variables are independent. Then it can be shown that

$$\mathbf{E}(\min\{k_1, k_2\}) = \frac{1}{2}\lambda - \frac{1}{2}e^{-\lambda} \sum_{k=0}^{\infty} k \left[\left(\frac{1}{3}\right)^{k/2} + 3^{k/2} \right] \mathbf{I}_k\left(\frac{\sqrt{3}}{2}\lambda\right), \quad (12)$$

where \mathbf{I}_k is the modified Bessel function of the first kind. As λ increases, the probability distribution function (pdf) of $\min\{k_1, k_2\}$ approaches the pdf of k_1 , and the expected value approaches $\lambda/4$ from below, which makes sense because the relative spacing of the random variables (relative to their standard deviations) increases, and we effectively have $\min\{k_1, k_2\} \approx k_1$. However, in the beginning of the algorithm where the number of loops is small, the number of intersection events is relatively small due to the absence of existing weight contributions. In other words, the expected number of intersection events at any edge approaches $Np/4$, and the standard deviation of this number approaches $\sqrt{Np}/2$.

For an $n \times n$ RBM, it can be easily shown that $p = 4/n^2$, then the expected number of intersection events at a given edge follows the expression in Eq. (12) with parameter $\lambda = Np = \frac{4N}{n^2} = \frac{4\rho}{n}$, meaning that this expected value will approach $\lambda/4 = N/n^2$. The expected number of the total intersection events in the entire RBM is this times the total number of connections, or $\frac{N}{n^2}n^2 = N$, or simply the number of loops. This makes sense because in the limit of large N , all the weights are positive, so adding a new loop will guarantee an intersection event.

E. Maximum Frustration of $2 \times m$ Unbiased Gauged RBM

Consider a gauged $2 \times m$ RBM weight matrix. We can permute the rows and columns such that all the negative weight elements are concentrated on the upper left and lower right corner. We can divide the matrix into six blocks, $B_1 = 1 \times [[1, m_1]]$, $B_2 = 1 \times [[m_1 + 1, m_2]]$, $B_3 = 1 \times [[m_2 + 1, m]]$, $B_4 = 2 \times [[1, m_1]]$, $B_5 = 2 \times [[m_1 + 1, m_2]]$, $B_6 = 2 \times [[m_2 + 1, m]]$ such that all the negative weight elements are in the B_1 and B_6 blocks.

Note that a column cannot contain more than one negative element, otherwise the positive-sum condition will be violated, so no negative elements can exist inside the B_3 and B_4 blocks, and we also require that $m_2 > m_1$ so that the negative elements are ‘‘separated’’ by columns containing only positive elements. Note also that we cannot have $m_1 = m_2$, otherwise $B_1 \cup B_6$ will constitute a vertex-switching subset whose sum is negative. Finally, if we apply the positive-sum condition to each row, then we see that the magnitude of every element in B_4 must be greater than the magnitude of the corresponding element in B_1 of the same column. Similarly, the magnitude of every element in B_5 must be greater than the magnitude of the corresponding element in B_6 of the same column. This condition can be expressed as

$$\sum_{w \in B_4} w \geq \sum_{w \in B_1} |w|, \quad \sum_{w \in B_5} w \geq \sum_{w \in B_6} |w|. \quad (13)$$

Let us now look at the vertex-switching subset that contains exactly one element from every column. To ensure that the

matrix satisfies the positive-sum condition, it is sufficient to select the smallest element from each column to form the vertex-switching subset of the smallest sum and force that sum to be non-negative (which implies that every vertex-switching subset must have a non-negative sum). This obviously implies that this subset should contain every element in B_1 and every element in B_6 . Without loss of generality, we can also assume that every element in B_2 is smaller than the corresponding element in B_5 of the same column, or

$$\sum_{w \in B_5} w \geq \sum_{w \in B_2} w. \quad (14)$$

Then the smallest sum is given by the sum of all the elements in the set $B_1 \cup B_2 \cup B_6$. Since B_2 contains only positive elements, and B_1 and B_6 contain only negative elements, this implies

$$\sum_{w \in B_2} w \geq \sum_{w \in B_1 \cup B_6} |w|. \quad (15)$$

Combining Equations 13, 14, and 15, we get the following relationship

$$\begin{aligned} & \sum_{ij} |W_{ij}| \\ &= \sum_{w \in B_1} |w| + \sum_{w \in B_2} |w| + \sum_{w \in B_3} |w| \\ & \quad + \sum_{w \in B_4} |w| + \sum_{w \in B_5} |w| + \sum_{w \in B_6} |w| \\ &= \left(\sum_{w \in B_1} |w| + \sum_{w \in B_4} |w| \right) + \left(\sum_{w \in B_2} |w| + \sum_{w \in B_5} |w| \right) \\ & \quad + \left(\sum_{w \in B_3} |w| + \sum_{w \in B_6} |w| \right) \\ &\geq 2 \sum_{w \in B_1} |w| + 2 \sum_{w \in B_2} |w| + 2 \sum_{w \in B_6} |w| \\ &\geq 2 \sum_{w \in B_1} |w| + 2 \sum_{w \in B_1 \cup B_6} |w| + 2 \sum_{w \in B_6} |w| \\ &\geq 4 \sum_{w \in B_1 \cup B_6} |w|. \end{aligned}$$

In other words, the sum of the absolute value of all weight elements must be four times greater than the sum of the absolute value of all the negative weight elements. Therefore, we see from Eq. (6) that the frustration index is bounded from above by 0.25.

F. Generating a 2×3 gauged RBM

We first look at the negation of statement (9)

$$\begin{aligned} & \text{If } \mathbf{y} \text{ satisfies } \mathbf{L}^T \mathbf{y} \geq 0 \text{ and } \mathbf{y} \geq 0, \\ & \text{then it must also satisfy } \mathbf{w}^T \mathbf{y} \geq 0. \end{aligned} \quad (16)$$

The goal is to prove this statement to be true for a 2×3 gauged RBM weight matrix \mathbf{w} . There are 12 possible loop atoms for the system: 4 for the leftmost 2×2 block, 4 for the rightmost 2×2 block, and 4 for the union of the leftmost and

rightmost column. Let us first look at the leftmost loop **I**, and try to see what $\mathbf{1}^T \mathbf{y}$ implies

$$l_{11}y_{11} + l_{21}y_{21} + l_{12}y_{12} + l_{22}y_{22} \geq 0.$$

Of the four loop edges $\{l_{11}, l_{12}, l_{21}, l_{22}\}$, we can assign one of them -1 and the rest $+1$, this gives us four inequalities

$$\begin{aligned} y_{11} + y_{21} + y_{12} &\geq y_{22}, \\ y_{21} + y_{12} + y_{22} &\geq y_{11}, \\ y_{12} + y_{22} + y_{11} &\geq y_{21}, \\ y_{22} + y_{11} + y_{21} &\geq y_{12}. \end{aligned}$$

If we assume that y_{22} is the maximum of the four y values, or $y_{22} = \max\{y_{11}, y_{12}, y_{21}, y_{22}\}$, then only the following inequality has to be satisfied

$$y_{11} + y_{21} + y_{12} \geq y_{22}.$$

It is easy to check that the other three inequalities are automatically satisfied since the y values are non-negative. In short, this means that whenever the y values form a ‘‘loop’’, the largest y element of this loop must be greater than the sum of the three other elements. This applies also for the other two loops.

We now turn our attention to the gauged RBM weight matrix \mathbf{w} . Without loss of generality we can assume that the two negative elements in the \mathbf{w} matrix are w_{11} and w_{12} . Note that there cannot be more than two negative elements in a 2×3 gauged RBM, and we can always permute the matrix such that the two negative elements are at the upper-left corner. Then the following must hold due to the positive-sum condition (ignoring the inequalities that are trivially true)

$$\begin{aligned} w_{11} + w_{21} &\geq 0, & w_{12} + w_{22} &\geq 0, \\ w_{11} + w_{12} + w_{13} &\geq 0, & w_{11} + w_{12} + w_{23} &\geq 0. \end{aligned}$$

This implies the following relationship

$$\begin{aligned} & \mathbf{w}^T \mathbf{y} \\ &= w_{11}y_{11} + w_{12}y_{12} + w_{13}y_{13} + w_{21}y_{21} + w_{22}y_{22} + w_{23}y_{23} \\ &\geq y_{11}w_{11} + y_{12}w_{12} + y_{13}(-w_{11} - w_{12}) \\ & \quad + y_{21}(-w_{11}) + y_{22}(-w_{12}) + y_{23}(-w_{11} - w_{12}) \\ &\geq -w_{11}(y_{13} + y_{21} + y_{23} - y_{11}) \\ & \quad -w_{12}(y_{13} + y_{22} + y_{23} - y_{12}) \\ &\geq 0, \end{aligned}$$

since $w_{11} \leq 0$ and $w_{12} \leq 0$ by construction, and $y_{13} + y_{21} + y_{23} \geq y_{11}$ and $y_{13} + y_{22} + y_{23} \geq y_{12}$. Therefore, we have shown that statement (16) must be true, and thus we can generate any gauged 2×3 RBM with loop atoms.

G. Local Minima

Consider n independent identical random variables $\{x_1, x_2, \dots, x_n\}$ with the following probability mass function

$$P(x_i = -\alpha) = \frac{1}{4} \quad P(x_i = 1) = \frac{3}{4}.$$

Let us partition the random variables into two subsets, with the first subset containing the first n_1 variables, and the

second containing the last $n_2 = n - n_1$ variables. Let n_{1+} be the number of random variables in the first subset with value $+1$, and let $n_{1-} = n_1 - n_{1+}$ be the number of random variables with value $-\alpha$ (note that both n_{1+} and n_{1-} are random variables themselves). Then the sum of all the random variables in the first subset can be expressed as $n_{1+} - \alpha n_{1-} = n_1 - (\alpha + 1)n_{1-}$. Note that n_{1-} follows a binomial distribution with mean $\frac{1}{4}n_1$ and variance $\frac{3}{16}n_1$. If we assume that the size of the subset is large enough so the central limit theorem applies, then the sum follows a normal distribution with

$$\begin{aligned}\mathbf{E}(n_1 - (1 + \alpha)n_{1-}) &= \frac{1}{4}(3 - \alpha)n_1, \\ \text{var}(n_1 - (1 + \alpha)n_{1-}) &= \frac{3}{16}(\alpha + 1)^2 n_1.\end{aligned}$$

Similarly for the sum of the second subset, which also follows a normal distribution with

$$\begin{aligned}\mathbf{E}(n_2 - (1 + \alpha)n_{2-}) &= \frac{1}{4}(3 - \alpha)n_2, \\ \text{var}(n_2 - (1 + \alpha)n_{2-}) &= \frac{3}{16}(\alpha + 1)^2 n_2.\end{aligned}$$

Since the difference of two normal random variables is still a normal random variable, the difference between the sum of the first subset and the sum of the second subset follows a normal distribution with mean $\frac{1}{4}(3 - \alpha)(n_1 - n_2)$ and variance $\frac{3}{16}(\alpha + 1)^2(n_1 + n_2)$, and the probability that this difference is greater than zero is

$$\begin{aligned}P((n_1 - 2n_{1-}) - (n_2 - 2n_{2-}) \geq 0) \\ &= \frac{1}{2}\left(1 + \text{erf}\left(\frac{\mu}{\sqrt{2}\sigma}\right)\right) \\ &= \frac{1}{2}\left(1 + \text{erf}\left(k(\alpha)\frac{n_1 - n_2}{\sqrt{6n}}\right)\right),\end{aligned}$$

where erf denotes the error function, and $k(\alpha) = \frac{3-\alpha}{\alpha+1}$. We see that this probability approaches $1/2$ asymptotically as n increases, with the direction of approach determined by the sign of $n_1 - n_2$.

Now, we consider a gauged biased RBM with weight matrix \mathbf{W} . Let \mathbf{s} be some arbitrary spin state, and without loss of generality assume that the corresponding switching subset is $F = ([n_1 + 1, n + 1] \times [1, m_1]) \cup ([1, n_1] \times [m_1 + 1, m + 1])$, where $n_1 \leq n$ and $m_1 \leq m$. In other words, the switching subset is the just the upper-right quadrant of some partition of the weight matrix, plus the lower-left quadrant. If the state \mathbf{s} is a local minimum, then the following condition has to be satisfied

$$\begin{aligned}\sum_{j=1}^{m_1} W_{ij} - \sum_{j=m_1+1}^{m+1} W_{ij} &\geq 0 \quad \forall i \in [[1, n_1]], \\ \sum_{j=m_1+1}^{m+1} W_{ij} - \sum_{j=1}^{m_1} W_{ij} &\geq 0 \quad \forall i \in [[n_1 + 1, n + 1]], \\ \sum_{i=1}^{n_1} W_{ij} - \sum_{i=n_1+1}^{n+1} W_{ij} &\geq 0 \quad \forall i \in [[1, m_1]], \\ \sum_{i=n_1+1}^{n+1} W_{ij} - \sum_{i=1}^{n_1} W_{ij} &\geq 0 \quad \forall i \in [[m_1 + 1, m + 1]].\end{aligned}$$

If we make the approximation that the partial sum over a row and the partial sum over a column is independent (which is justified because the correlation between the two sums is only due to one single element at the intersection), then the probability that all the above conditions are satisfied is

$$\begin{aligned}p(n_1, m_1) &= \frac{1}{2^{n+m+2}} \left(1 + \text{erf}\left(k\frac{2m_1 - m - 1}{\sqrt{6(m+1)}}\right)\right)^{n_1} \\ &\quad \left(1 + \text{erf}\left(k\frac{m+1 - 2m_1}{\sqrt{6(m+1)}}\right)\right)^{n+1-n_1} \\ &\quad \left(1 + \text{erf}\left(k\frac{2n_1 - n - 1}{\sqrt{6(n+1)}}\right)\right)^{m_1} \\ &\quad \left(1 + \text{erf}\left(k\frac{n+1 - 2n_1}{\sqrt{6(n+1)}}\right)\right)^{m+1-m_1}.\end{aligned}$$

Note that there are $\binom{n}{n_1}$ ways to flip n_1 spins in the visible layer and $\binom{m}{m_1}$ ways to flip m_1 spins in the hidden layer. If we further choose to ignore the potential correlations between the local minima, then the expected number of local minima of an $n \times m$ RBM is given by

$$\sum_{n_1=0}^n \sum_{m_1=0}^m p(n_1, m_1) \binom{n}{n_1} \binom{m}{m_1} - p(0, 0),$$

where the reason to subtract $p(0, 0)$ is to discount the planted global optimum being a trivial local minimum.

It can be shown empirically that this value scales poorly with the system size and $k(\alpha)$. In other words, it is difficult for local minima to populate the energy landscape for a large RBM instance generated using random loops. It is also difficult for local minima to populate the energy landscape when the frustration index is small (corresponding to a smaller α value or larger k value).

H. Ability to Generate Local Minima with the Structured Loop Algorithm

Again, we consider the vertex-switching subset $F = B_1 \cup B_4$. The goal is to show that the state corresponding to F satisfies the inequality conditions for being a local minimum (Eq. (7)) by a relatively large margin, so that any states that are ‘‘close’’ to this state are also likely to be local minima. Since the structured frustrated-loop algorithm we propose is invariant under a matrix transpose, we only have to focus on verifying the local minimum conditions by looking at each individual rows, corresponding to the first two conditions in Eq. (7)

$$\sum_J W_{ij} \geq \sum_{J^c} W_{ij} \quad \forall i \in I \quad \sum_{J^c} W_{ij} \geq \sum_J W_{ij} \quad \forall i \in I^c, \quad (17)$$

and a similar analysis will follow for the last two conditions in Eq. (7). To make the notations less cumbersome, we denote $B_1 = I \times J^c$, $B_2 = I \times J$, $B_3 = I^c \times J^c$, and $B_4 = I \times J^c$.

We first look at some row $i \in I$, which we can divide into two halves: half of it in B_1 (J), and half of it in B_2 (J^c). And we let the sums of the elements in the two individual halves be S_{i1} and S_{i2} , respectively. Furthermore, let N_{i1} , N_{i2} , and N_{i3} be the number of left loops, upper loops, and center loops with vertices in row i , respectively. Note that each left

loop contributes $-(1-\alpha)$ units energy to S_{i1} ; each upper loop contributes either $+\alpha$ or -1 units energy to S_{i1} and contributes -1 unit of energy to S_{i2} ; each center loop contributes $+\alpha$ units of energy to S_{i1} and -1 unit of energy to S_{i2} . Then we have the following

$$\begin{aligned} N_{i1}(\alpha - 1) + N_{i3}(1 + \alpha) &\leq S_{i2} - S_{i1} \\ &\leq N_{i1}(\alpha - 1) + (N_{i2} + N_{i3})(1 + \alpha). \end{aligned} \quad (18)$$

We then see that the condition to guarantee that F corresponds to a local minimum is

$$N_{i1}(\alpha - 1) + N_{i3}(\alpha + 1) \geq 0 \implies \frac{N_{i3}}{N_{i1}} \geq \frac{1 - \alpha}{1 + \alpha}, \quad (19)$$

which is always true for all $\alpha \in [0, 1]$ if we force $N_{i3} \geq N_{i1}$ for all rows i , and we see that the first inequality in expression (17) will be satisfied by a large margin.

Similarly, if we look at some row $i \in I^c$ and divide it into a half in B_3 and a half in B_4 , and denote S_{i3} and S_{i4} as the sums over the two respective halves, then an upper loop will not contribute to either sum; a left loop will have a -2 energy contribution to S_{i3} ; and a center loop will have a -1 energy contribution to both S_{i3} and S_{i4} . Then we have the following

$$S_{i3} - S_{i4} = 2N_{i1} \geq 0,$$

which implies that the second inequality in expression (17) will be satisfied by a large margin.

A similar discussion will apply to the last two conditions in Eq. (7) (by looking at each individual column), except now we require $N_{j3} \geq N_{j2}$ for all columns j to guarantee a local minimum. Therefore, we see that for a sufficiently large number of center loops, the likelihood of the conditions $N_{i3} \geq N_{i1}$ and $N_{j3} \geq N_{j2}$ being satisfied is relatively high, implying that we will have a high population of local minima.

I. Simulated Annealing

We start by assigning the following probability to each node/spin state energy

$$p(\beta, s) = e^{-\beta E(s)},$$

where β can be interpreted as the inverse temperature of the system. The simulated annealing algorithm can be thought of as a Metropolis-Hastings sampling algorithm on a probability mass function varying in time (based on the β schedule). Recall that the acceptance ratio for the Metropolis-Hastings algorithm is

$$A(s, s') = \min\left(1, \frac{p(s')}{p(s)}\right) = \min\left(1, e^{-E(s') + E(s)}\right).$$

We call an iteration of the simulated annealing algorithm a *sweep*. A sweep consists of performing single-spin flips over all the spins in the visible layer, then performing spin flips over the hidden layer. Solving a non-trivial RBM instance usually requires multiple sweeps. Since this is a single-spin flip algorithm, we restrict our focus to the energy difference of a single spin flip. Recall that the RBM energy is

$$E(v, h) = -\left(\sum_{ij} W_{ij} v_i h_j + \sum_i a_i v_i + \sum_j b_j h_j\right),$$

so we can express the energy difference of a single spin flip in the visible layer as

$$\begin{aligned} &-E(v'_i, h) + E(v_i, h) \\ &= a_i(v'_i - v_i) + \sum_j W_{ij}(v'_i - v_i)h_j \\ &= 2v'_i(a_i + \sum_j W_{ij}h_j) \\ &= 2v'_i\theta_i(h), \end{aligned}$$

where $v'_i = -v_i$ and we define $\theta = \mathbf{W}h$. Similarly, we express the energy difference of a single spin flip in the hidden layer as

$$-E(v, h'_j) + E(v, h_j) = 2h'_j\phi_j(h),$$

where we define $\phi = \mathbf{W}^T v$. Then, the acceptance ratio can be written as:

$$\begin{aligned} A(v'_i, v_i) &= \min(1, e^{2\beta v'_i\theta_i}), \\ A(h'_j, h_j) &= \min(1, e^{2\beta h'_j\phi_j}). \end{aligned}$$

If the total number of sweeps for a given run is N_{sweep} , we can then set β according to the following linearly increasing schedule:

$$\beta = \beta_{min} + \frac{c-1}{N_{sweep}-1}(\beta_{max} - \beta_{min}),$$

where β_{min} is the minimum value of β for this run, and β_{max} is the maximum value of β . We provide a basic pseudo-code for the simulated annealing algorithm in Algorithm 3, where the angle updates for a single spin flip are given by

$$\begin{aligned} \Delta\theta_j &= W_{ij}(h'_j - h_j) = 2W_{ij}h'_j, \\ \Delta\phi_i &= W_{ij}(v'_i - v_i) = 2W_{ij}v'_i. \end{aligned}$$

Algorithm 3 Simulated Annealing on RBMs

- 1: Initialize a random spin configuration $\mathbf{v}^{(0)}, \mathbf{h}^{(0)}$
 - 2: $\theta^{(0)} = \mathbf{W}\mathbf{h}^{(0)}, \phi^{(0)} = \mathbf{W}^T\mathbf{v}^{(0)}, E^{(0)} = E(\mathbf{v}^{(0)}, \mathbf{h}^{(0)})$
 - 3: **for** $c \in [1, N_{sweep}]$ **do**
 - 4: $\beta = \beta_{min} + (\beta_{max} - \beta_{min})\frac{c-1}{N_{sweep}-1}$
 - 5: **for** $i \in [1, n]$ **do**
 - 6: $v_i = -v_i, A = \min(1, e^{2\beta v_i\theta_i^{(c-1)}})$
 - 7: **if** $rand() < A$ **then**
 - 8: Get new $\phi^{(c)}, E^{(c)}$
 - 9: **else**
 - 10: $v_i = -v_i$
 - 11: **for** $j \in [1, m]$ **do**
 - 12: $h_j = -h_j, A = \min(1, e^{2\beta h_j\phi_j^{(c-1)}})$
 - 13: **if** $rand() < A$ **then**
 - 14: Get new $\theta^{(c)}, E^{(c)}$
 - 15: **else**
 - 16: $h_j = -h_j$
-

Assuming that m scales linearly with n , then the size of the RBM (total number of spins) is of the order $O(n)$. Note that flipping a single spin requires updating the entire θ or ϕ vector, so the time complexity of performing a single spin update is $O(n)$. Since performing a sweep requires flipping all the spins of the RBM, the time complexity of a single sweep is $O(n^2)$.

J. Optimal Sweep Schedule

For a given triplet of the parameters $\{n, f, \rho\}$, it is possible to generate multiple random RBM instances. The distribution of the total numbers of sweeps N_{tot} required to solve the instances follows approximately a log-normal distribution. If we have k samples of N_{tot} , we can estimate the log mean of N_{tot} to be $\hat{\mu} = \frac{1}{k} \sum_{i=1}^k N_{tot,i}$, and the log standard deviation to be $\hat{\sigma} = \sqrt{\frac{1}{k-1} \sum_{i=1}^k (N_{tot,i} - \hat{\mu})^2}$. We can then estimate the approximate 95th percentile of the distribution of N_{tot} to be

$$N_{tot,95\%} = \exp(\hat{\mu} + 2\hat{\sigma}).$$

From now on, the 95 percentile is assumed when we refer to N_{tot} .

To ensure that we are not overestimating N_{tot} for the generated instance and thus its difficulty, we have to ensure that we use the optimal sweep schedule N_{sweep} for any given n and f . The optimization of N_{sweep} is performed in two stages. In the first stage, we perform the optimization without the knowledge of the hardest loop density $\rho(n)$, so N_{sweep} is not necessarily optimized to solve the hardest instances. However, using this non-optimal N_{sweep} , we can nonetheless locate the hardest loop densities for various n , since the hardness peak is rather insensitive to N_{sweep} (see Section VI-B). After locating the hardness peaks, we move on to the second stage of the optimization, where we set ρ such that it corresponds to the hardest instances for a given n . This allows us to perform a second iteration of optimization on N_{sweep} such that it is tuned to solve the hardest instances.

In the first stage of optimization, we fix the loop density at $\rho = 0.47$ and let $n \in \{30, 40, 50, 60, 70, 80\}$ and $f \in \{0.05, 0.075, 0.1, 0.125, 0.15, 0.175\}$ so the instances are easy enough to be solved within a reasonable amount of time. For each pair of $\{n, f\}$, we generate 10000 different RBM instances, and try to solve them with varying N_{sweep} , and find the optimal N_{sweep} that minimizes the 95th percentile of N_{tot} . We fit the relationship between the optimal N_{sweep} and $\{n, f\}$ with a product of two polynomials with respect to the two parameters, and find the data to be well fitted by the following function:

$$N_{sweep} = (0.504n^2 - 13.3n + 311) \\ \times (193f^3 - 52.7f^2 + 4.73f - 0.102).$$

This sweep schedule is used to perform the hardness peak study in Section VI-B. To find the scaling behavior of N_{sweep} for instances generated at the hardest loop densities, we perform a similar procedure, but instead of fixing ρ at some constant value, we let $\rho(n)$ be a function of n such that it corresponds to the hardest instances at every n . We then arrive at the following fitting function

$$N_{sweep} = (1.29n^2 - 33.1n + 1664) \\ \times (41.4f^3 - 11.7f^2 + 1.06f - 0.018).$$

This sweep schedule is used to perform the frustration study in Section VI-C.

REFERENCES

- [1] M. W. Krentel, "The complexity of optimization problems," *Journal of computer and system sciences*, vol. 36, no. 3, pp. 490–509, 1988.
- [2] M. Lewin, D. Livnat, and U. Zwick, "Improved rounding techniques for the max 2-sat and max di-cut problems," in *International Conference on Integer Programming and Combinatorial Optimization*. Springer, 2002, pp. 67–82.
- [3] M. R. Garey, D. S. Johnson, and L. Stockmeyer, "Some simplified np-complete problems," in *Proceedings of the sixth annual ACM symposium on Theory of computing*. ACM, 1974, pp. 47–63.
- [4] Z. Bian, F. Chudak, W. G. Macready, and G. Rose, "The ising model: teaching an old problem new tricks," *D-wave systems*, vol. 2, 2010.
- [5] J. Cheriyan, W. Cunningham, L. Tuncel, and Y. Wang, "A linear programming and rounding approach to max 2-sat," *DIMACS series in discrete mathematics and theoretical computer science*, vol. 26, pp. 395–414, 1996.
- [6] M. R. Garey, D. S. Johnson, and L. Stockmeyer, "Some simplified np-complete problems," in *Proceedings of the sixth annual ACM symposium on Theory of computing*. ACM, 1974, pp. 47–63.
- [7] T. Dimitriou, "Sat distributions with planted assignments and phase transitions between decision and optimization problems," *Discrete applied mathematics*, vol. 153, no. 1–3, pp. 58–72, 2005.
- [8] O. Watanabe and M. Yamamoto, "Average-case analysis for the max-2sat problem," in *International Conference on Theory and Applications of Satisfiability Testing*. Springer, 2006, pp. 277–282.
- [9] I. Hen, J. Job, T. Albash, T. F. Ronnow, M. Troyer, and D. A. Lidar, "Probing for quantum speedup in spin-glass problems with planted solutions," *Physical Review A*, vol. 92, no. 4, p. 042325, 2015.
- [10] K. Xu and W. Li, "Many hard examples in exact phase transitions," *Theoretical Computer Science*, vol. 355, no. 3, pp. 291–302, 2006.
- [11] D. B. West *et al.*, *Introduction to graph theory*. Prentice hall Upper Saddle River, NJ, 1996, vol. 2.
- [12] A. Fischer and C. Igel, "An introduction to restricted boltzmann machines," in *iberamerican congress on pattern recognition*. Springer, 2012, pp. 14–36.
- [13] R. Durrett, *Probability: theory and examples*. Cambridge university press, 2019, vol. 49.
- [14] N. Srivastava and R. R. Salakhutdinov, "Multimodal learning with deep boltzmann machines," in *Advances in neural information processing systems*, 2012, pp. 2222–2230.
- [15] C. J. Geyer, "Markov chain monte carlo maximum likelihood," 1991.
- [16] H. Tjelmeland and B. K. Hegstad, "Mode jumping proposals in mcmc," *Scandinavian journal of statistics*, vol. 28, no. 1, pp. 205–223, 2001.
- [17] C. Sminchisescu and M. Welling, "Generalized darting monte carlo," *Pattern Recognition*, vol. 44, no. 10–11, pp. 2738–2748, 2011.
- [18] S. Lan, J. Streets, and B. Shabbaba, "Wormhole hamiltonian monte carlo," in *Twenty-Eighth AAAI Conference on Artificial Intelligence*, 2014.
- [19] S. Kullback and R. A. Leibler, "On information and sufficiency," *The annals of mathematical statistics*, vol. 22, no. 1, pp. 79–86, 1951.
- [20] H. Manukian, Y. R. Pei, and M. Di Ventra, "Optimal unsupervised learning of restricted boltzmann machines," In preparation.
- [21] M. Mézard, G. Parisi, and M. Virasoro, *Spin glass theory and beyond: An Introduction to the Replica Method and Its Applications*. World Scientific Publishing Company, 1987, vol. 9.
- [22] S. Aref, A. J. Mason, and M. C. Wilson, "An exact method for computing the frustration index in signed networks using binary programming," *arXiv preprint arXiv:1611.09030*, 2016.
- [23] I. P. Gent and T. Walsh, "The sat phase transition," in *ECAI*, vol. 94. PITMAN, 1994, pp. 105–109.
- [24] T.-D. Lee and C.-N. Yang, "Statistical theory of equations of state and phase transitions. ii. lattice gas and ising model," *Physical Review*, vol. 87, no. 3, p. 410, 1952.
- [25] Y. R. Pei, "Loop-algorithm," <https://github.com/PeaBrane/Loop-Algorithm.git>, 2019.
- [26] S. Arora and B. Barak, *Computational Complexity: A Modern Approach*. Cambridge University Press, 2009.
- [27] E. Boros, P. L. Hammer, and G. Tavares, "Local search heuristics for quadratic unconstrained binary optimization (qubo)," *Journal of Heuristics*, vol. 13, no. 2, pp. 99–132, 2007.
- [28] J. E. Whitesitt, *Boolean algebra and its applications*. Courier Corporation, 1995.
- [29] R. B. Griffiths, "Correlations in ising ferromagnets. ii. external magnetic fields," *Journal of Mathematical Physics*, vol. 8, no. 3, pp. 484–489, 1967.

- [30] M. N. Ellingham, "Vertex-switching, isomorphism, and pseudosimilarity," *Journal of graph theory*, vol. 15, no. 6, pp. 563–572, 1991.
- [31] G. F. Simmons, *Introduction to topology and modern analysis*. Tokyo, 1963.
- [32] E. F. Krause, *Taxicab geometry: An adventure in non-Euclidean geometry*. Courier Corporation, 1986.
- [33] T. Jech, *Set theory*. Springer Science & Business Media, 2013.
- [34] J. Elliott and P. Dawber, *Symmetry in Physics, Volume 1 and 2*. Macmillan, 1979.
- [35] R. Balian, J. Drouffe, and C. Itzykson, "Gauge fields on a lattice. ii. gauge-invariant ising model," *Physical Review D*, vol. 11, no. 8, p. 2098, 1975.
- [36] F. R. K. Chung, R. L. Graham, and R. M. Wilson, "Quasi-random graphs," *Combinatorica*, vol. 9, no. 4, pp. 345–362, 1989.
- [37] A. Blass, G. Exoo, and F. Harary, "Paley graphs satisfy all first-order adjacency axioms," *Journal of Graph Theory*, vol. 5, no. 4, pp. 435–439, 1981.
- [38] J. Banavar, M. Cieplak, and M. Muthukumar, "Dynamics of frustrated spin clusters," *Journal of Physics C: Solid State Physics*, vol. 18, no. 7, p. L157, 1985.
- [39] W. Fenchel and D. W. Blackett, *Convex cones, sets, and functions*. Princeton University, Department of Mathematics, Logistics Research Project, 1953.
- [40] S. N. Chiu, D. Stoyan, W. S. Kendall, and J. Mecke, *Stochastic geometry and its applications*. John Wiley & Sons, 2013.
- [41] D. Solow, "Linear and nonlinear programming," *Wiley Encyclopedia of Computer Science and Engineering*, 2007.
- [42] K. Paton, "An algorithm for finding a fundamental set of cycles of a graph," *Communications of the ACM*, vol. 12, no. 9, pp. 514–518, 1969.
- [43] J. C. Tiernan, "An efficient search algorithm to find the elementary circuits of a graph," *Communications of the ACM*, vol. 13, no. 12, pp. 722–726, 1970.
- [44] R. Tarjan, "Enumeration of the elementary circuits of a directed graph," *SIAM Journal on Computing*, vol. 2, no. 3, pp. 211–216, 1973.
- [45] D. B. Johnson, "Finding all the elementary circuits of a directed graph," *SIAM Journal on Computing*, vol. 4, no. 1, pp. 77–84, 1975.
- [46] P. Mateti and N. Deo, "On algorithms for enumerating all circuits of a graph," *SIAM Journal on Computing*, vol. 5, no. 1, pp. 90–99, 1976.
- [47] Y. LeCun, Y. Bengio, and G. Hinton, "Deep learning," *nature*, vol. 521, no. 7553, p. 436, 2015.
- [48] R. Salakhutdinov and G. Hinton, "Deep boltzmann machines," in *Artificial intelligence and statistics*, 2009, pp. 448–455.
- [49] S. Kirkpatrick, C. D. Gelatt, and M. P. Vecchi, "Optimization by simulated annealing," *science*, vol. 220, no. 4598, pp. 671–680, 1983.
- [50] J. L. Hennessy and D. A. Patterson, *Computer architecture: a quantitative approach*. Elsevier, 2011.
- [51] L. De Rose, K. Gallivan, E. Gallopoulos, B. Marsolf, and D. Padua, "Falcon: A matlab interactive restructuring compiler," in *International Workshop on Languages and Compilers for Parallel Computing*. Springer, 1995, pp. 269–288.
- [52] V. Kumar, *Introduction to parallel computing*. Addison-Wesley Longman Publishing Co., Inc., 2002.
- [53] M. R. Garey and D. S. Johnson, *Computers and Intractability: A Guide to the Theory of NP-Completeness*. New York, NY, USA: W. H. Freeman & Co., 1990.
- [54] S. R. White, "Concepts of scale in simulated annealing," in *AIP Conference Proceedings*, vol. 122, no. 1. AIP, 1984, pp. 261–270.
- [55] R. J. Hyndman and Y. Fan, "Sample quantiles in statistical packages," *The American Statistician*, vol. 50, no. 4, pp. 361–365, 1996.
- [56] C. C. Heyde, "On a property of the lognormal distribution," *Journal of the Royal Statistical Society: Series B (Methodological)*, vol. 25, no. 2, pp. 392–393, 1963.
- [57] S. Sachdev, "Quantum phase transitions," *Handbook of Magnetism and Advanced Magnetic Materials*, 2007.
- [58] S. Chen, L. Wang, S.-J. Gu, and Y. Wang, "Fidelity and quantum phase transition for the heisenberg chain with next-nearest-neighbor interaction," *Physical Review E*, vol. 76, no. 6, p. 061108, 2007.
- [59] G. E. Hinton, "Training products of experts by minimizing contrastive divergence," *Neural computation*, vol. 14, no. 8, pp. 1771–1800, 2002.
- [60] J. H. Friedman, "Stochastic gradient boosting," *Computational statistics & data analysis*, vol. 38, no. 4, pp. 367–378, 2002.
- [61] R. Salakhutdinov, "Learning deep boltzmann machines using adaptive mcmc," in *Proceedings of the 27th International Conference on Machine Learning (ICML-10)*, 2010, pp. 943–950.
- [62] F. Pérez-Cruz, "Kullback-leibler divergence estimation of continuous distributions," in *2008 IEEE international symposium on information theory*. IEEE, 2008, pp. 1666–1670.
- [63] D. H. Wolpert, W. G. Macready *et al.*, "No free lunch theorems for optimization," *IEEE transactions on evolutionary computation*, vol. 1, no. 1, pp. 67–82, 1997.
- [64] I. Stoianov, M. Zorzi, S. Becker, and C. Umiltà, "Associative arithmetic with boltzmann machines: The role of number representations," in *International Conference on Artificial Neural Networks*. Springer, 2002, pp. 277–283.
- [65] D. Erhan, Y. Bengio, A. Courville, P.-A. Manzagol, P. Vincent, and S. Bengio, "Why does unsupervised pre-training help deep learning?" *Journal of Machine Learning Research*, vol. 11, no. Feb, pp. 625–660, 2010.
- [66] A. Coates, A. Ng, and H. Lee, "An analysis of single-layer networks in unsupervised feature learning," in *Proceedings of the fourteenth international conference on artificial intelligence and statistics*, 2011, pp. 215–223.
- [67] R. Shwartz-Ziv and N. Tishby, "Opening the black box of deep neural networks via information," *arXiv preprint arXiv:1703.00810*, 2017.
- [68] J. Argelich, C.-M. Li, F. Manyà, and J. Planes, "The first and second max-sat evaluations," *Journal on Satisfiability, Boolean Modeling and Computation*, vol. 4, pp. 251–278, 2008.
- [69] R. H. Swendsen and J.-S. Wang, "Nonuniversal critical dynamics in monte carlo simulations," *Physical review letters*, vol. 58, no. 2, p. 86, 1987.
- [70] U. Wolff, "Collective monte carlo updating for spin systems," *Physical Review Letters*, vol. 62, no. 4, p. 361, 1989.
- [71] R. H. Swendsen and J.-S. Wang, "Replica monte carlo simulation of spin-glasses," *Physical review letters*, vol. 57, no. 21, p. 2607, 1986.
- [72] Z. Zhu, A. J. Ochoa, and H. G. Katzgraber, "Efficient cluster algorithm for spin glasses in any space dimension," *Physical review letters*, vol. 115, no. 7, p. 077201, 2015.
- [73] B. Molnár and M. Ercsey-Ravasz, "Analog dynamics for solving max-sat problems," in *2014 14th International Workshop on Cellular Nanoscale Networks and their Applications (CNNA)*. IEEE, 2014, pp. 1–2.
- [74] F. L. Traversa and M. Di Ventra, "Polynomial-time solution of prime factorization and np-complete problems with digital memcomputing machines," *Chaos: An Interdisciplinary Journal of Nonlinear Science*, vol. 27, p. 023107, 2017.
- [75] F. Traversa, P. Cicotti, F. Sheldon, and M. Di Ventra, "Evidence of an exponential speed-up in the solution of hard optimization problems," *Complexity*, vol. 2018, no. 7982851, 2018.
- [76] F. Sheldon, F. L. Traversa, and M. Di Ventra, "Taming a non-convex landscape with dynamical long-range order: memcomputing the ising spin-glass," *arXiv preprint arXiv:1810.03712*, 2018.